TECHNICAL MEMORANDUM

691

# Volcanic sulphur dioxide plume forecasts based on UV-satellite retrievals for the 2011 Grímsvötn and the 2010 Eyjafjallajökull eruption


Johannes Flemming and Antje Inness

Research Department


December 2012

to be submitted to JGR




European Centre for Medium-Range Weather Forecasts
Europäisches Zentrum für mittelfristige Wettervorhersage
Centre européen pour les prévisions météorologiques à moyen

Series: ECMWF Technical Memoranda

A full list of ECMWF Publications can be found on our web site under:
http://www.ecmwf.int/publications/

Contact: library@ecmwf.int

**Abstract**

The sulphur dioxide plumes released by the eruptions of the Icelandic volcanoes Eyjafjallajökull in May 2010 and Grímsvötn in May 2011 were studied using observations from GOME-2, OMI and SCIAMACHY and modelled with the Integrated Forecasting System (IFS) of ECMWF. The satellite retrievals of $SO_2$ total columns (TCSO2) were (i) used to estimate source strength and injection height of the two eruptions and (ii) assimilated by the IFS to obtain initial conditions for subsequent forecasts. The observed plume location agreed well between the retrievals from the different instruments but only GOME-2 observations provided complete spatial coverage. The source strength was deduced from the observations within the area covered by the plume simulations. The applied methodology led to emission estimates of 0.25 Tg over a period of 25 days in May 2010 and 0.32 Tg over 2 days in 2011. The injection height was assessed by finding the largest overlap between the observed plume and an ensemble of plume forecasts injected at different levels. GOME-2 TCSO2 retrievals were assimilated with ECMWF's 4D-VAR algorithm to provide the initial conditions for plume forecasts. The $SO_2$ analyses captured the plume maxima well but exaggerated the plume area. Plume forecasts were evaluated by means of hit-rate and plume-size statistics for different TCSO2 thresholds. Plume forecasts using either the source parameters only or the initial conditions only agreed reasonably with the observations but using both led to the best forecast performance. The initialisation improved in particular the forecast of the Grímsvötn plume several days after the end of the eruption. The correctness of the injection height was crucial during the eruption of Grímsvötn because of a pronounced vertical wind shear. The developed forecast and assimilation system can be applied for near-real-time forecasting of volcanic $SO_2$ plumes.

# 1 Introduction

The severe implications for the aviation industry during the eruption of Eyjafjallajökull volcano (63.63 N, 19.62 W, 1666 m a.s.l.) from 14 April - 23 May 2010 instigated a strong research effort in the areas of transport modelling as well as ground- and space based remote sensing and in-situ aircraft observation. Roughly a year later, on 21 May 2011, the Grímsvötn volcano (64.42 N, 17.33 W, 1725 m a.s.l.) started emitting large amounts of ash and $SO_2$ over two days, which affected North-European airspace for three days. The official end of this eruption was announced for 28 May 2011.

Volcanic $SO_2$ is considered to be a proxy for volcanic ash, in particular for the finest ash size fraction in young plumes. Further, conversion of $SO_2$ to sulphate is the cause for secondary aerosol formation in the plume, which itself poses a risk for aviation [*Carn et al. 2009, Thomas and Prata, 2011*]. Hence, forecast and observation of volcanic $SO_2$ could provide useful guidance for the aviation industry during volcanic eruptions. In this paper we present a forecast system for $SO_2$ that exploits information provided by UV-VIS satellite retrievals of total column $SO_2$ (TCSO2). We infer emissions parameters from TCSO2. We also use the observations to initialise and therefore correct forecasts during and after the eruption. We apply the method to the 2011 eruption of Grímsvötn and the second phase of the 2010 Eyjafjallajökull eruption starting on 1 May 2010.

The ash plume of the Eyjafjallajökull eruption in 2010 is well documented in the scientific literature. The predicted movement of the ash plume by different models agrees well with satellite imagery and ground based observations [*Emeis et al. 2010, Stohl et al. 2011,* and *Dacre et al. 2011*]. T*homas and Prata* [*2011*] investigate the relation between ash and $SO_2$ during the Eyjafjallajökull eruption. They find mostly a good correspondence between ash retrievals from the SEVIRI instrument and $SO_2$ retrievals from AIRS and IASI. In the aged plume $SO_2$ and ash are separated because of different removal mechanisms. *Schumann et al.* [*2010*] carry out 17 research flights between 19 April and 18 May 2010. The observed ash and $SO_2$ layers are located between 1 and 7 km altitude. They are 0.3 to 3 km deep and typically 100 to 300 km wide. *Schumann et al.* [*2010*] report a pronounced correlation between ash, $SO_2$ and CO in the plume. They explain increased concentrations of observed aerosol in the Aitken mode with the conversion of $SO_2$ to sulphuric acid. *Bukowiecki et al.* [*2011*] come to same conclusion for the in-situ observations at Jungfrau-Joch. *Heue et al.* [*2011*] report a good correlation between $SO_2$, BrO and ash. The $SO_2$ plume was detected by OMI, AIRS [*Thomas and Prata, 2011*] and GOME-2 [*Heue et al., 2011, Rix et al., 2012*]. *Rix et al.* [*2012*] also provide estimates of the $SO_2$ plume height based on the GOME-2 retrieval. *Heard et al.* [*2012*] model the $SO_2$ with the NAME model [*Dacre et al. 2011*] using emissions estimated from IASI $SO_2$ retrievals. Since no $SO_2$ source profile was available, $SO_2$ was released uniformly up to 10 km in their study.

Fewer papers have been published to date on the 2011 Grímsvötn eruption but its 2004 eruption has been used for model inter-comparison of dispersion models [*Witham, et al., 2007*]. *Kerminen et al.* [*2011*] and *Tesche et al.* [*2012*] characterise the ash plume over Scandinavia with surface observation and satellite retrievals as well as transport modelling. *Kerminen et al.* [*2011*] report the separation of the ash from the $SO_2$ plume based on OMI retrievals but can not resolve the observed differences with their modelling system. The ash-plume travelled toward Scandinavia, whereas the $SO_2$ was transported towards Greenland.

Retrievals of volcanic TCSO2 can be made from infra-red (IR) instruments such as AIRS [*Prata and Bernardo, 2007*] , IASI [*Clarisse et al. 2008*] and ACE [*Doeringer et al. 2012*] as well as from ultra violet (UV) sensors such as TOMS [*Krueger et al. 1995*], OMI [*Krotkov et al. 2006,Yang et al. 2007*], SCIAMACHY [*Lee et al. 2008, 2009*], GOME [*Eisinger et al. 1998*] and GOME-2 [*Rix et al. 2009*]. These TCSO2 retrievals rely on an assumption about the plume height and are therefore often issued for different assumed altitudes of the plume. First steps have been made to also infer the plume height estimates by *Yang et al.* [*2009*] and *Rix et al.* [*2012*]. The $TCSO_2$ retrievals are limited to the overpass times, which make it difficult to capture the pronounced temporal variability of the plumes. The underlying retrievals algorithms are uncertain in the presence of clouds, high albedo or low thermal contrast.

Satellite $SO_2$ retrievals from various instruments can differ considerably, which makes it worthwhile to consider not only one instrument. *Lee et al.* [2009] compare OMI and SCIAMACHY $SO_2$ and find good agreement with respect to location of the plume but the actual retrieved maximum values and instantaneous $SO_2$ load can vary up to a factor of 2-3 and the obtained total emitted $SO_2$ mass by up to 50%. *Thomas and Prata et al.,* [*2011*] conclude that the $SO_2$ tonnage from OMI is about two times bigger than the one retrieved from AIRS retrievals in May 2010. *Van Geffen et al.* [*2008*] report good agreement in the plume location between GOME-2 and SCIAMACHY but find differences of about 30 DU (50%) in the observations of the $SO_2$ plume of the Kasatochi volcano in August 2008. *Kristiansen et al.* [*2010*] review estimates of the Kasatochi emissions, which vary from 1.2 to 2.5 Tg based on retrievals from GOME-2, OMI, AIRS and IASI.

Source strength and injection height are important parameters for the correct simulation of the volcanic $SO_2$ or ash plume. During the eruptions of Grímsvötn and Eyjafjallajökull the maximum height of the emitted ash plume was monitored with a radar by the Icelandic Meteorological Office. The release height of $SO_2$ is however not necessarily the same as the one for ash. *Mastin et al.* [*2009*] suggest an empirical formula of the relation between plume height and emitted ash. It was used to estimate ash emissions in 2010 and 2011 by the UK met-office and other modelling groups [*C. Whitman, personal communication*]. *Stohl et al.* [2011] provide an improved estimate of injection height and emitted ash for Eyjafjallajökull based on inversing modelling using satellite observations. The relation between the emitted mass and the eruption strength as indicated by the injection height seems to be highly variable. Likewise, there is no constant relation between the emission factors for ash, fine particles or $SO_2$.

Because of the limited knowledge of emission height and $SO_2$ source strength, it seems worthwhile to exploit the satellite observations to infer the source terms. Satellite observations are often used to estimate the total $SO_2$ emission flux. *Krueger et al.* [*1995*] use the day-today change in the observed $SO_2$ burden to estimate the $SO_2$ fluxes. *Eckardt et al.* [*2008*] and *Kristiansen et al.* [*2010*] improve basic estimates of emissions flux and injection height by inverse modelling. *Hughes et al.* [*2012*] evaluate modelled trajectory in a statistical framework to estimate activity and injection height of the plume. We refine the approaches based on the observed $SO_2$ burdens, by using simulated transport patterns to improve the knowledge of the temporal variability of the emission flux estimate. Further, we use wind-shear from a meteorological model to identify the approximate height of the plume.

A complementary approach to the source estimate is the construction of initial tracer fields from satellite observations during the eruption. Data assimilation [*Daley, 1991*] is a well-established methodology to produce initial conditions for numerical weather prediction by combining model results with observations based on assumption about the error and representativeness characteristics of the model and observations. The advantage of the data assimilation approach is that observations of the plume can be used to correct the forecast during and after the eruption and thereby reduce the uncertainty introduced by the plume parameter estimate.

A system for retrospective and near-real-time data assimilation and forecasting of global atmospheric composition has been built at the ECMWF by extending the IFS with modules for atmospheric composition [*Hollingsworth et al. 2008*]. The Monitoring Atmospheric Composition and Climate (MACC) and MACC-II projects [http://www.gmes-atmosphere.eu/) provide reanalyses [*Inness et al. 2012*] and operational forecasts of atmospheric composition. Key species for the assimilations with the MACC system are ozone and CO and aerosol optical depth. The MACC system has been applied to assimilate and forecast volcanic aerosols [*Benedetti et al., 2012*] and we use it in this study to assimilate and forecast volcanic $SO_2$.

The paper is structured as follows. An overview of the instruments and the data quality procedures is given in section 2. The model and data assimilation system is presented in section 3. OMI, GOME-2 and SCIAMACHY observations for May 2009, 2010 and 2011 are discussed with respect to mean and maximum values as well as burdens and $SO_2$ lifetimes in section 4. Section 5 is dedicated to estimates of the source parameters injection height and emission flux. The evaluation of the analyses and forecasts of the $SO_2$ plumes is the content of section 6. The paper is concluded with a discussion and summary in sections 7 and 8.

## 2 TCSO2 Satellite observations

$SO_2$ observations by UV instruments are possible because $SO_2$ has strong absorption in the wavelength range of 306-340 nm. This range of the spectrum is otherwise dominated by ozone absorption. The comparison of the UV observations with calculated radiances which take ozone into account is the general principle of the $SO_2$ retrieval. The retrieval algorithm of TCSO2 from UV radiance observations consists of three steps: (i) the spectral retrieval of the slant SO2 column, (ii) the correction with respect to the atmospheric background levels of $SO_2$ and (iii) the conversion of the slant columns to vertical TCSO2 using air mass factors.

### 2.1 OMI

The OMI instrument on board the EOS-AURA satellite measures in the range between 270-500 nm with a spectral resolution of 0.5 *nm* [*Levelt et al., 2006*]. The 2600 km wide OMI swath contains 60 pixels of which the smallest pixel, i.e. at nadir position, has a size of 13x24 km. AURA’s equatorial crossing time is 13.30. The viewing zenith angle is up to 65°. The operational TCSO2 retrievals for the troposphere and stratosphere (OMSO2 V.111), which were used in this study, are processed with the fast Linear Fit (LF) algorithm [*Yang et al. 2007*]. The differences at ten wavelengths in the range 308.7 – 375 nm between measured and computed UV radiances that account only for ozone, Ring-effect (i.e. “filling-in” of Fraunhofer lines in scattered sunlight) and surface reflectivity are used to infer TCSO2 concentrations. The LF algorithm is optimized for the retrieval of volcanic $SO_2$. The OMI ozone retrievals (OMTO3) are used as the computed estimate for ozone. The LF $SO_2$ algorithm is sensitive to the assumed height of the SO2 plume because this influences the air mass factor, which is needed for the conversion of slant columns into vertical TC. The LF algorithm underestimates large TCSO2 > 100 DU [*Yang et al. 2009*]. The level 2 data used in this study were obtained from http://disc.sci.gsfc.nasa.gov/Aura/data-holdings/OMI/omso2_v003.shtml

## 2.2 GOME-2

The Second Global Ozone Monitoring Experiment (GOME-2) is a nadir-scanning UV-VIS spectrometer aboard of the MetOp-A platform, which crosses the equator at 9:30. The spectral resolution varies between 0.26 nm and 0.51 nm in the range of 240-790 nm. The size of the field of view is 80 km x 40 km over the full scan. With a swath width of 1920 km global coverage is achieved in about 1.5 days. A comprehensive description of the GOME-2 $SO_2$ retrievals is given in *Rix at al.* [*2012*]. The slant column fit for the SO2 retrievals applies differential optical absorption spectroscopy [DOAS, Platt, 1994]. It is performed in the UV wavelength range between 315 – 326 nm [*Thomas et al., 2005*]. To minimize interference with ozone absorption a correction is applied to the $SO_2$ slant column values [*Valks et al., 2011*]. The GOME Data Processor (GDP) version 4.4 [*Valks et al., 2011*] is used for the air mass factor calculations. The operational GOME-2 TCSO2 products are provided by the German Aerospace Centre (DLR) in the framework of EUMETSAT's Satellite Application Facility on Ozone and Atmospheric Chemistry Monitoring (O3M-SAF).

## 2.3 SCIAMACHY

The SCIAMACHY instrument was payload of the Envisat satellite. The operation of Envisat ended on 8 April 2012. Envisat crossed the equator at 10.00 local time [*Bovensmann et al., 1998*]. SCIAMACHY observed alternating in nadir and limb viewing geometry in the spectral range between 220-2400 nm at a resolution of 0.25 – 0.4 nm. The swath with in nadir position was 1000km and the pixels size was 60x30 km. Global coverage was achieved in 6 day. The viewing zenith angle was between 5-20°. SCIAMACHY channel 2 (310-405nm) in nadir viewing geometry is used to obtain $SO_2$ retrievals either with a standard DOAS or a weighting function (WF) DOAS [*Lee et al., 2008*]. WFDOAS retrievals account better for the wavelength dependence of the ozone air mass factor and include an improved treatment of the ring effect. The level-2 $SO_2$ retrievals from SCIAMACHY were produced by BIRA for the PROMOTE project (http://www.gse-promote.org).

## 2.4 Quality control and data height selection

Table 1 summarises the TCSO2 satellite retrievals products from the OMI, SCIAMACHY and GOME-2 used in this study. The operational usage of satellite retrievals requires quality control procedures to filter out data of low quality. The retrieval quality, expressed as a quality flag, might have been compromised by the presence of clouds, at low solar elevation, or by technical issues with the instrument. The OMI instrument suffers from "row anomalies", which affects the right half of the swath, i.e. cross-track pixels 53-54 and 27-44 in the period of the April – May 2010 and May 2011. Based on the documentation (http://www.knmi.nl/omi/research/product/rowanomaly-background.php) and *Krotkov* [*personal communication*] it was decided to apply a stricter filter conditions and to use only cross-track pixels smaller than 25. The quality control procedure reduced the number of pixels in the 9-15 UTC time window over the considered region by a factor of about 5 for the OMI data whereas the number pixel from SCIAMACHY and GOME-2 was not significantly reduced.

The retrievals for all instruments are provided for assumed plume heights in the lower troposphere (trl), the middle troposphere (trm) and the lower stratosphere (stl). The corresponding height for these levels is given in table 1. Only the trm and stl levels are likely heights for plumes from active eruptions of the volcanic explosivity indices 3 (Eyjafjallajökull) and 4 (Grímsvötn) [Newhall and Self, 1982]. To investigate the differences between trm and stl TCSO2 retrievals, Figure 1 shows scatter diagrams of the daily 50% (median) and the 99 % (P99) percentile of the pixel values for stl and trm for the days during and after the 2010 and 2011 eruption. There was a good linear relation between stl and trl for both median and P99. The medians of the stl retrievals from OMI and GOME-2 tended to be about 5% lower than the trm retrieval whereas the stl SCIAMACHY retrievals were about 5% higher than trm retrievals. The P90 and P99 values of stl were up to 10-20 % lower than trm, in particular for OMI because the stl plume height is 2 – 3 km higher than the respective height for SCIAMACHY and GOME-2. The location of the observed pixels did not differ between stl and trm for all satellites. Given the small differences between stl and trm retrievals, we decided to use only the trm retrievals for the remainder of this paper.

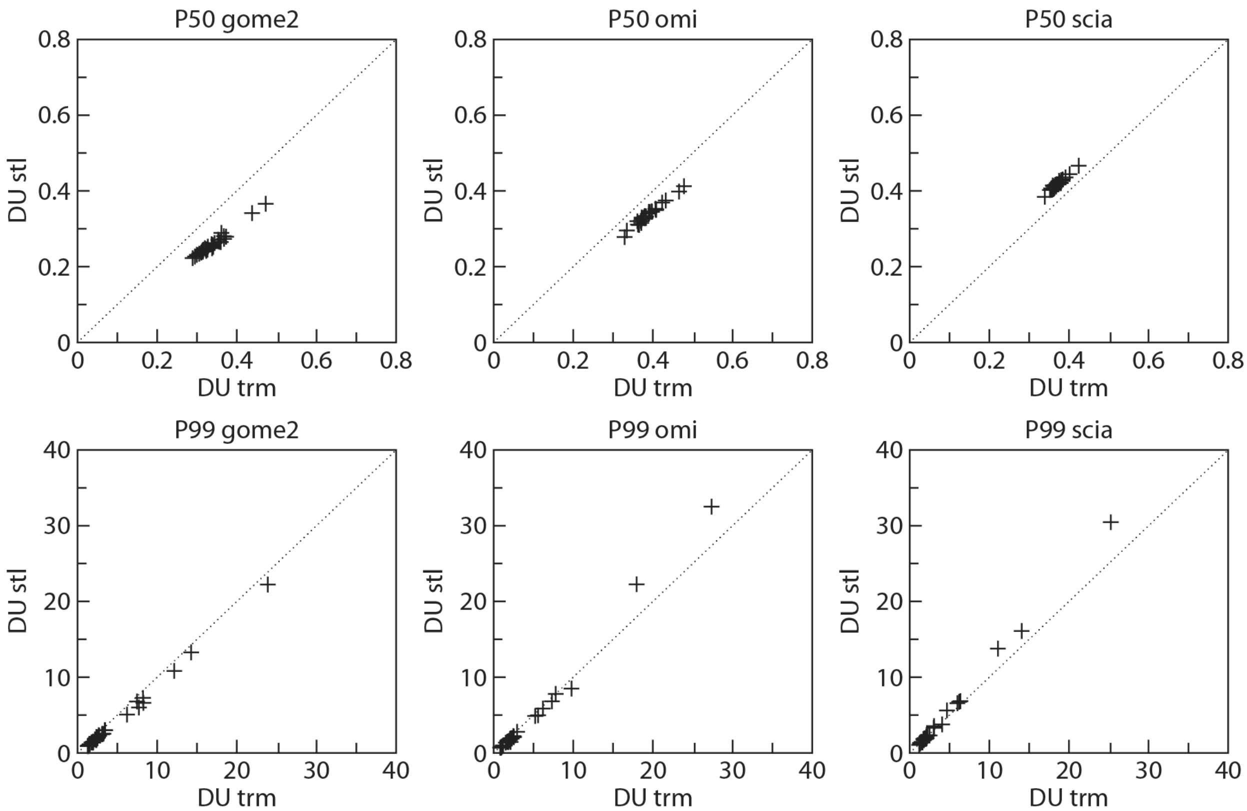


*Figure 1 TCSO2 retrievals (DU) valid for an assumed plume height in the middle troposphere (trm, x-axis) and the lower stratosphere (stl, y-axis) for the daily median (P50, top) and the 99%-Percentile (P99, bottom) in the periods 5-23 May 2010 and 22-31 May 2011 from GOME-2 (left), OMI (middle) and SCIAMACHY (right).*

| Instrument | Producer, code | over pass time | Quality Control | Level height trl, trm, stl | Website |
|---|---|---|---|---|---|
| OMI | NASA, L2 | 13:30 | SOE >10°, FOV < 25, chi-square < 1 | 2.5, 7.5, 17 km | http://disc.sci.gsfc.nasa.gov/Aura/data-holdings/OMI/omso2_v003.shtml |
| SCIAMACHY | BIRA,L2 | 10:00 | SOE >20°, QF =0 | 1, 6, 14 km | http://www.gse-promote.org/ |
| GOME-2 | DLR, L2 | 9:30 | SOE >25°, QF = 0 | 2.5, 6, 15 km | http://wdc.dlr.de/data_products/SERVICES/GOME2NRT/so2.php |

*Table 1 List of TCSO2 satellite products used. (QF, quality flag, SOE: solar elevation angle, FOV: field of view)*

# 3 $SO_2$ Model and assimilation system

## 3.1 Model

Volcanic $SO_2$ is represented as a transported tracer in the IFS, which is subject to wet deposition and chemical loss expressed as constant e-folding time. The IFS uses a semi-lagrangian advection scheme and a proportional global mass fixer was applied to ensure exact mass conservation. The forecasts and analyses were carried out at a horizontal resolution of about 40 km (TL511). The model had 60 vertical levels with a top at 0.1 hPa. The vertical model resolution between 5-15 km height was about 0.5 to 1 km. The corresponding model time step was 900 s. In our study, the lifetime was set to a fixed value of 10 days. The height of the orography in T511 resolution is 1444 m at the location of Grímsvötn and 660 m of Eyjafjallajökull.

The choice of the $SO_2$ life time is an important parameter in this study even though the uncertainty introduced by the emissions is greater than the uncertainty due to the lifetime over the forecast period of a few days. The $SO_2$ lifetime because of reaction with OH varies in the atmosphere. The lifetime decreases with height and is assumed to be of the order of 10 days in the middle and upper troposphere based on CTM model results. The lifetime is considerably longer in the stratosphere because OH concentrations are smaller since water vapour concentrations are low. *Eckardt et al.* [*2008*] and *Kristiansen et al.* [*2010*] apply a lifetime based on a modelled OH climatology. The $SO_2$ variable introduced in IFS for aerosol modelling varies with latitude from 3 days in the tropics to 8 days in the polar region [*Morcrette et al., 2009*].It should be noted that the conditions in a plume are most likely different from the situation in the clean troposphere, which makes it difficult to assume climatological OH levels. *Schuman et al.* [*2010*] observed in-situ a collocated increase in $SO_2$, CO and volcanic ash as well as strongly reduced ozone levels. The lack of sun-light and reduced ozone could indicate lower than normal OH concentrations. *Krotkov et al.* [*2010*] estimate an e-folding time of 8-9 days for the eruption of Kasatochi in 2008 based on OMI observations.

## 3.2 Assimilation system

In addition to producing forecasts the MACC system (which is based on the IFS) can assimilate concentration fields of reactive gases [*Inness et al, 2012, Flemming et al. 2011*] and aerosols [*Benedetti et al. 2009*], which are more continuously distributed than volcanic $SO_2$ plumes. The MACC system only changes the concentration fields according to observations and does not modify the underlying emissions.

The MACC system applies ECMWF's incremental formulation of the four-dimensional variational data assimilation (4D-Var) method [*Mahfouf and Rabier, 2000*]. In ECMWFs 4D-Var, a cost function is minimized over a time window of 12 hours in such a way that the resulting analysis is an optimal combination of the model fields and the observations based on the prescribed background error and observation error statistics.

The assimilation of volcanic $SO_2$ plumes challenges the assumption about Gaussian error characteristics of model and observation errors made in data assimilation. The algorithm for the assimilation of volcanic $SO_2$ has to cope with the fact that the observed values of the volcanic $SO_2$ are extreme maximum values and that the assimilating mode1 provides a poor first guess if no volcanic source is included.

A volcanic plume is a singular event since the $SO_2$ concentrations can change suddenly by 2 to 3 orders of magnitude. This makes it difficult to calculate background error statistics with the NMC method [*Parrish and Derber 1992*] as used for several other fields in the MACC system, e.g. CO, or the analysis ensemble method [*Fisher 2004, 2006*], which was used for the estimate of the ozone background errors at ECMWF.

Therefore, background error statistics for volcanic $SO_2$ were constructed by prescribing a background error standard deviation profile and a structure function with a length scale of 100 km for the horizontal correlations, and by assuming a diagonal vertical correlation matrix. The standard deviation profile had a constant default value of $1.0^{-10}$ kg/kg which was increased to $1.0^{-7}$ kg/kg where the plume was estimated to be based on the plume injection height estimate (see section 5). The observation errors statistics were taken from the errors provided by the data producers.

# 4 TCSO2 retrievals over Iceland in May 2009-2011

We studied the different TCSO2 retrievals (trm) around Iceland for May of the years 2009 to 2011. The study area was a circle centred around Iceland with a radius of 2000 for the mean and high value statistics. For the calculation of total burdens a larger study area of 4000 km was used in order to minimise the influence of the movement of the plume in to and out of the study area on the budget. The great majority of the orbits in the 4000 km area occur between 9 and 15 UTC. The Aura (OMI), Envisat (SCIAMACHY) and MetOP-A (GOME-2) satellites passed over the study area about 3 to 4 times providing about 4800 (OMI), 2500 (SCIAMACHY) and 3500 (GOME-2) valid pixels. To illustrate the different viewing characteristics, TCSO2 retrievals for 7 May 2010 from all instruments are shown in Figure 2. Only GOME-2 provides valid observations for the whole area with a regular coverage. OMI and SCIAMACHY show considerable gaps due to the observing geometry or the quality control. In particular, the invalidity of many OMI observations because of its row anomaly (see section 2.4) requires cautious interpretation of the plume extent and any statistical parameters of the plume. Because of the converging orbits, the coverage by OMI and SCIAMACHY improves north of Iceland. The observations of the 2011 eruption of Grímsvötn benefit from this because in 2011 the $SO_2$ plume moved mainly north of Iceland whereas in 2010 the Eyjafjallajökull plume was often located south of Iceland.

To harmonise the different retrievals, which differed in pixels size, coverage and overpass time, we mapped the pixels to a gridded data set of 0.5° x 0.25° resolution for each day. The gridded data set was produced by calculating the average of the pixel observations in each grid box allowing a spatial tolerance of half a grid box for extrapolation. Grid boxes without observations were given the median value of the pixels for that day, which was mostly in the range of 0.3 – 0.5 DU. The percentage of these average grid boxes, which occurred more often in the south, was about 15% for GOME-2 and about 50% for OMI and SCIAMACHY.

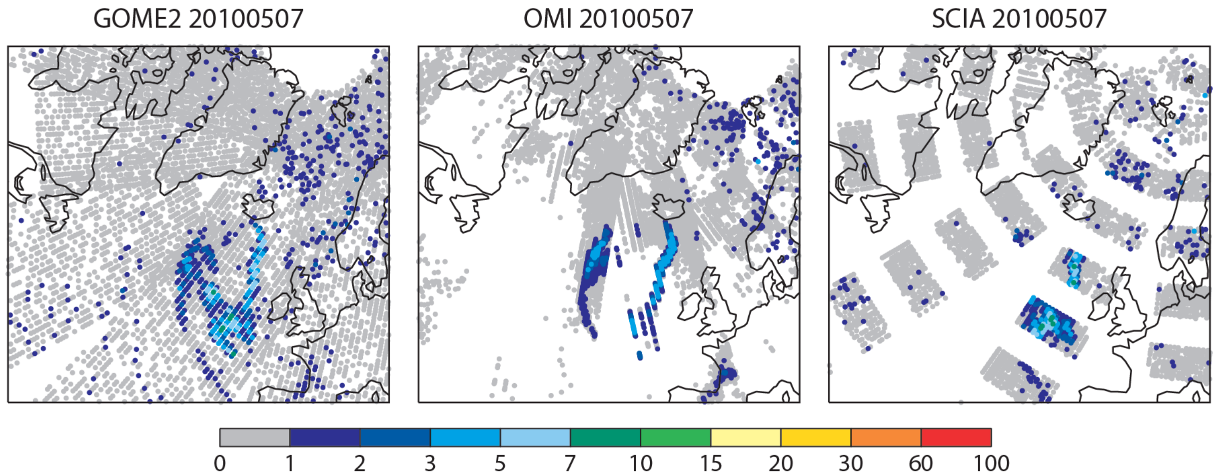


*Figure 2 TCSO2 retrievals on 7 May 2010 (80W-40E, 40N-80N) from GOME-2 (left), OMI (middle) and SCIAMACHY (right).*

### 4.1 Median and high values during and after the eruption

We analysed median and 99% -percentile (P99) of the gridded TCSO2 values over an area up to 2000 km around Iceland for May 2010 and mid-May to mid-June 2011 as well as for 2009 to relate the volcanic $SO_2$ plumes to the conditions without a volcanic eruption.

The median (see Figure 3, top) in May 2009 was about 0.3, 0.4 and 0.5 DU for SCIAMACHY, OMI and GOME-2 retrievals respectively and showed only little temporal variation. The eruptions raised the median to 0.5 DU for GOME-2 in 2010 but did not change the median of the OMI and SCIAMACHY retrievals. In 2011 the median for the gridded SCIAMACHY and GOME-2 retrievals was raised to 1 DU about 10 days after the eruption, whereas SCIAMACHY showed a weaker response. The reduction of the median from GOME-2 at the beginning of June 2011 was slower than for OMI. The noticeable increase of the median in 2011 proves that the Grímsvötn eruption had a significant impact on TCSO2 in the North Atlantic region.

A good indication of the $SO_2$ plume was P99, which is shown in Figure 3 for May 2009, 2010 and mid-May to mid- June 2011. All instruments had a P99 of about 1.25 DU in 2009. The highest P99 values were 2-3 time times higher during the eruption of Eyjafjallajökull and 20-30 times higher during eruption of Grímsvötn. The highest individual pixels were above 20 DU in May 2010 for all instruments and about 100 DU for GOME-2 and SCIAMACHY as well as 150 DU for OMI in May 2011.

The first phase of the Eyjafjallajökull eruption in April 2010 had released only little $SO_2$ and consequently TCSO2 P99 was only slightly higher at the beginning of May 2010 than in 2009. On 5 May 2010 P99 TCSO2 started to increase. The highest values of 3.5 DU (GOME-2) to 3 DU (OMI and SCIAMACHY) were reached from 7-9 May and decreased until the 12 May after which a second maximum (3DU) occurred from 13-18 May 2010.

The eruption of Grímsvötn in May 2011 started on 21 May at 18 UTC and quickly released large amounts of $SO_2$, which led to observed OMI P99 values of about 30 DU from 22-24 May. These values were about ten times as high as the observed maximum values during the Eyjafjallajökull eruption. SCIAMACHY and GOME-2 observed high values of 30 and 25 DU respectively only on 23 May. The P99 values of all instruments were strongly reduced on 25 May 2011. Circulated $SO_2$ from the start of the eruption entered the study area again leading to high P99 on 26 May. According to the visual and radar observations [*C. Whitam personal communication*] and the TCSO2 observations by all instruments Grímsvötn had stopped to emit significant amount of ash by 24 May. The official end of the eruption was declared to be on the morning of 28 May, and values returned to normal by 3 June 2011.

All instruments recorded a similar temporal development during the eruption but there were large differences on the day-to-day variability. Many of these differences were due to the less complete coverage of by OMI and SCIAMACHY. For instance, GOME-2 and SCIMACHY observed increased TCSO2 already on 5 May 2010, whereas OMI only observed it a day later because two orbits, which would have covered the plume on that day were missing in the data set. However, non-linear biases between the instruments may also play a role in explaining the differences for the median and the maximum values.

Figure 4 shows scatter plots of collocated gridded observations for both eruptions. The comparison only considers grid boxes with valid observations without regarding the differences in the overpass time. For the moderate TCSO2 values in 2010 the OMI values tend to be lower than the observations from GOME-2 and SCIAMACHY. In contrast, the OMI observations of the more intense plume in 2011 (with TCSO2 exceeding 20 DU in 2011) exceed the corresponding SCIAMACHY and OMI values by a factor of two. This can not only be explained by the smaller pixel size of the OMI instrument because the data have been mapped to the same grid resolution. GOME-2 and SCIAMACHY show smaller differences in 2010 but GOME-2 tends to provide the lowest values for the 2011 eruption.

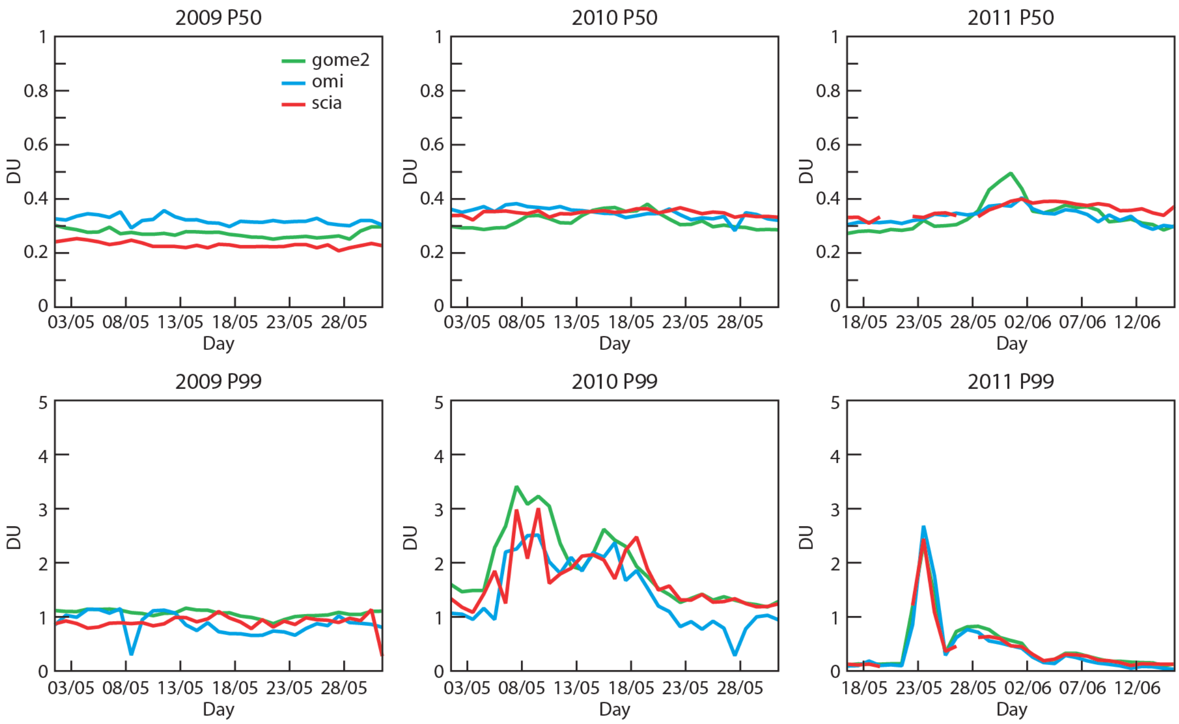


*Figure 3 Time series of the median (top) and the 99% percentile (bottom) of gridded TCSO2 retrievals by OMI, SCIAMACHY and GOME-2 over the North Western Atlantic (2000 km around Iceland) for May 2009 (left), 2010 (middle) and mid-May to mid-June 2011 (note the different scale of the vertical axis in the right panel).*

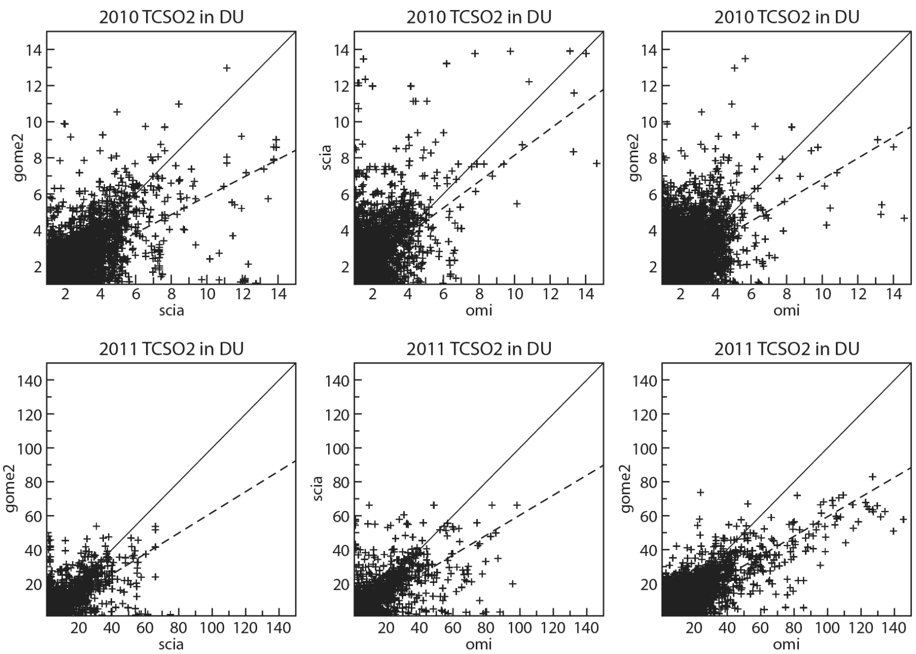


*Figure 4 Scatter plot of TCSO2 retrievals mapped to a 0.25° * 0.5 °grid of GOME-2 versus SCIAMACHY (left), SCIAMACHY versus OMI (middle) and GOME-2 versus OMI (right) for the periods 5-23 May 2010 (top) and 22-31 May 2011 (bottom). The dashed lines show a linear fit of the data. Only data greater 1 DU were considered.*

### 4.2 Total $SO_2$ burden

The change of the total $SO_2$ burden in the study area is caused by the emissions, the loss processes and transport in and out of the area. To avoid an increase of the burden in the study area because of a re-entering plume, the study area to estimate burdens was chosen to be a circle of 4000 km radius around Iceland, which covered all longitudes north of 80°N. The total $SO_2$ burden in the study area calculated from gridded GOME-2, OMI and SCIAMACHY retrievals is shown in Figure 5 (top). Figure 5 (bottom) displays day-to-day change in units of t/s, which is the unit of the emission source. Missing data for SCIAMACHY in 2011 led to larger gaps in the calculation of the day-to-day change.

In 2009, the year without eruption, the burden derived from the different instruments varied between the 0.45 and 0.55 Tg and the day-to-day variation of each instrument varied between +/- 0.3 t/s. Given the lack of a volcanic source in 2009, we attribute this variability mainly to random errors caused by the sampling characteristics of the satellites. 0.3 t/s is therefore a basic estimate of the expected random errors of the attempt to quantify the source strength from changes in the total burden.

During the eruption of Eyjafjallajökull, the burden was slightly raised by about 0.05-0.1 Tg compared to 2009. The change of $SO_2$ in 2010 was variable and mostly within the uncertainty range estimated from the observations in 2009. Only the GOME-2 observations suggested an effective source of up 0.5 t/s from 4-8 May 2010. Overall the eruption contributed very little to the $SO_2$ burden in the study area. In contrast, all instruments recorded an increase of the $SO_2$ burden by about 0.3 Tg over three days after the outbreak of the Grímsvötn in 2011. This increase corresponds to an effective source of 1.1 t/s from 21-24 May 2011.

The loss of $SO_2$ after the end of the emissions can be used to estimate the $SO_2$ lifetime, as demonstrated *by Krotkov et al.* [*2010*] for the Kasatochi eruption in 2008. The decrease of the $SO_2$ burden after the Grímsvötn eruption for all satellites did not fully follow an exponential decay. There was a large day-to-day variability and a linear loss would have been a better fit to the data than an exponential one. Nevertheless, a log-linear least square fit for the period from 24 May to 10 June assuming a background value of 0.5 Tg led to an e-folding time estimate of 8 days for OMI and of 14 days for GOME-2, which is in the expected range for the $SO_2$ lifetime. For both satellites the exponential loss model indicated an initial burden of about 0.1-0.15 Tg, i.e. about 50%, higher than the observed values on 24 May. The SCIAMACHY data showed a similar loss to OMI in the first three days after the end of the eruption but an increase later on, which did not seem to be caused by an $SO_2$ source but by sampling or instrument issues. Despite the large uncertainties in the estimate, the differences in the lifetimes based on OMI and GOME-2 is considerable. A possible explanation for discrepancy is the less complete coverage of OMI, which means that the median of pixels is used to fill the data gaps. The better spatial coverage made the GOME-2 observations less susceptible to sampling issues. Besides, GOME-2 and OMI have biases (Figure 3, top) when recording TCSO2 of lower intensity. Since the plume is rather widespread in early June 2011, these biases can influence the calculated $SO_2$ burdens.

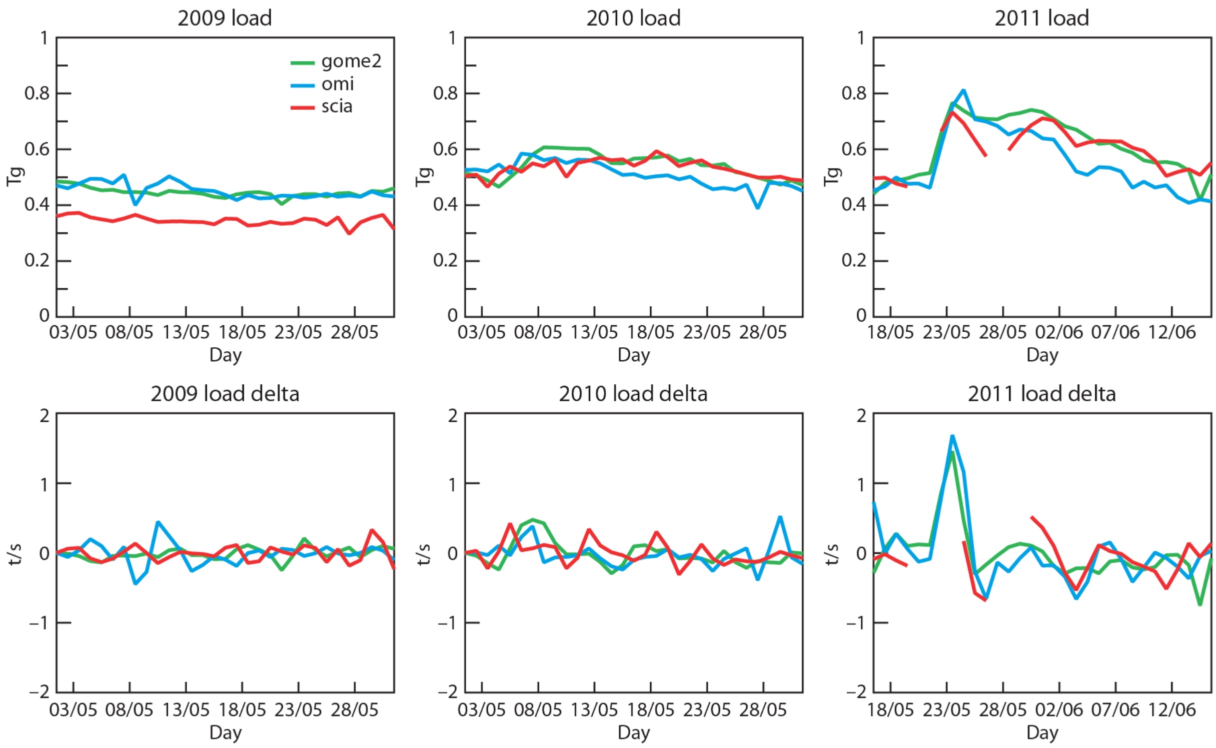


*Figure 5 Total $SO_2$ burden in Tg (top) and its day-to-day change in t/s (bottom) over an area of 4000 km surrounding Iceland for the years 2009, 2010 and 2011 from gridded daily observations of GOME-2, OMI and SCIAMACHY.*

# 5 Estimates of $SO_2$ source strength and injection height

The estimate of the emission source based on day-to-day differences of the observed $SO_2$ burden over a large area (see section 4.2) has uncertainties. In this section, we present a refined emission source as well as a height estimate, which uses additional information from plume simulations.

## 5.1 Description of method

Injection height and emission strength were based on the comparison of TCSO2 satellite observations with an ensemble of tracers, which were released at different heights. The test tracers were injected at vertical height intervals of about 2 – 3 km ranging from 2 to 15 km with a constant arbitrary emission strength of 1 t/s and an e-folding lifetime of 10 days. The choice of these plume height intervals was determined by the vertical resolution of the IFS model. The test tracers were injected into an atmosphere with zero tracer concentrations at the forecast start.

The method consisted of two steps: Firstly, the overlap between the plume shape of the test tracers and the observed plume was determined. A threshold of 1 DU, which is the climatological P99 value (see chapter 4.1) was applied to identify the plume in the observations. The injection height of the test tracer with the largest overlap was assumed to be the actual injection height. This step is based on the assumption that wind shear will lead to different plume shapes for different levels. If less than 10 % of the observed plume pixels (i.e. > 1 DU) were located within the modelled plume area, the corresponding plume was not considered to be a match with the observed plume. The end or pause of the emissions was assumed instead.

The second step was to determine the emission flux by calculating the ratio between the total SO$_2$ load of the test tracer plume with the best overlap and a gridded representation (see section 4.2) of the observations in the area of the test tracer plume. To identify the contribution from the volcano, the observations were reduced by the a background concentration value defined as the median of the observations (see section 4.1) This ratio was multiplied with the emissions flux used for the test tracers to obtain the emission flux estimate for the forecast period.

24 hour test tracer forecasts, started at 12 UTC, were used to determine the injection height average over a 24 h window in step 1. Only if the 24 hour forecast did not match sufficiently the observations, the forecasts with the shorter length were used to determine the plume height. Shorter forecast of 18, 12 and 6 h were used to further refine the height estimate in 2011.

## 5.2 Estimate for Grímsvötn in May 2011

A pronounced vertical wind shear was characteristic for the period of Grímsvötn eruption in 2011. Figure 6 (left) shows the GOME-2 observations and the 24 h test tracer forecasts after the eruption on 22 May. Table 2 contains the numerical data. The average wind speed was small but the lower plume was transported southwards whereas the higher plumes travelled northwards. The plume differences were more pronounced after a 72 h forecast as shown in Figure 7 for 24 May. Figure 8 shows the estimated emission flux (left) at a temporal resolution of 6 hours and the estimate of the injection height, together with the observations of the top plume height from a synoptic radar at Keflavik airport [*C. Witham personal communication*].

The estimated plume height centre was 12 km above orography for the first 18 hours of the eruption and dropped quickly to 6 km. The radar observed a plume top height between 15 and 20 km in the first 24 hours and about 11 km in the second 24 hours. The plume observations are the top height of the ash plume. It can be assumed that the emitted SO$_2$ reaches the upper parts of the ash plume because of the lack of gravitational settling. The plume height estimate corresponds to the plume centre and is therefore lower than the observed plume top height. The 72h forecasts of the test tracers (Figure 7) show that an injection height of 15 km and above would not have captured the observed plume section north of Scandinavia. Overall, there is a good correspondence between the estimate and the observed height, in particular for the second 24 hours.

The emission estimate, which was not restricted by the observed times of the eruption, led to the first emission in the 12-18 UTC time window on 21 May 2011. The actual start of the emissions was reported for 19 UTC. The estimated emissions increased quickly and reached the highest values of nearly 5 t/s from 12-18 UTC on 22 May. The observed plume top height indicates a less intensive ash injection with an average height of 5 km after 23 May, but the GOME-2 TCSO2 observation did not show any significant SO$_2$ plume from the source in this period, as shown in Figure 7 (left) for 24 May.

Small emissions of up to 0.2 t/s and lower were detected around 28 May 2011, i.e. after the end of the eruption had been declared. This emission estimate is an artefact caused by the transport of the plume back to the source region within 4-5 days. These derived fluxes are below the general uncertainty of emission estimates from total burdens of 0.3 t/s (see section 4.2).

Using OMI and SCIAMACHY observations led to similar estimates of the plume height for the first two days of eruption during which most of the $SO_2$ was emitted. However, the estimate of the emitted mass for the night of 22-23 May (18 UTC-6 UTC) was higher. The estimate based on OMI and on SCIAMACHY led to emission fluxes of about 8 and 6 t/s over 12 hours because of (i) the higher values of the observations within the plume for 23 May and (ii) the lack of observations in the area without a plume.

The majority of the Grímsvötn $SO_2$ emissions was released during the first two days of the eruption. The total $SO_2$ emissions were estimated to 0.39, 0.30 and 0.32 Tg based on the observations from OMI, SCIAMACHY and GOME-2 respectively.

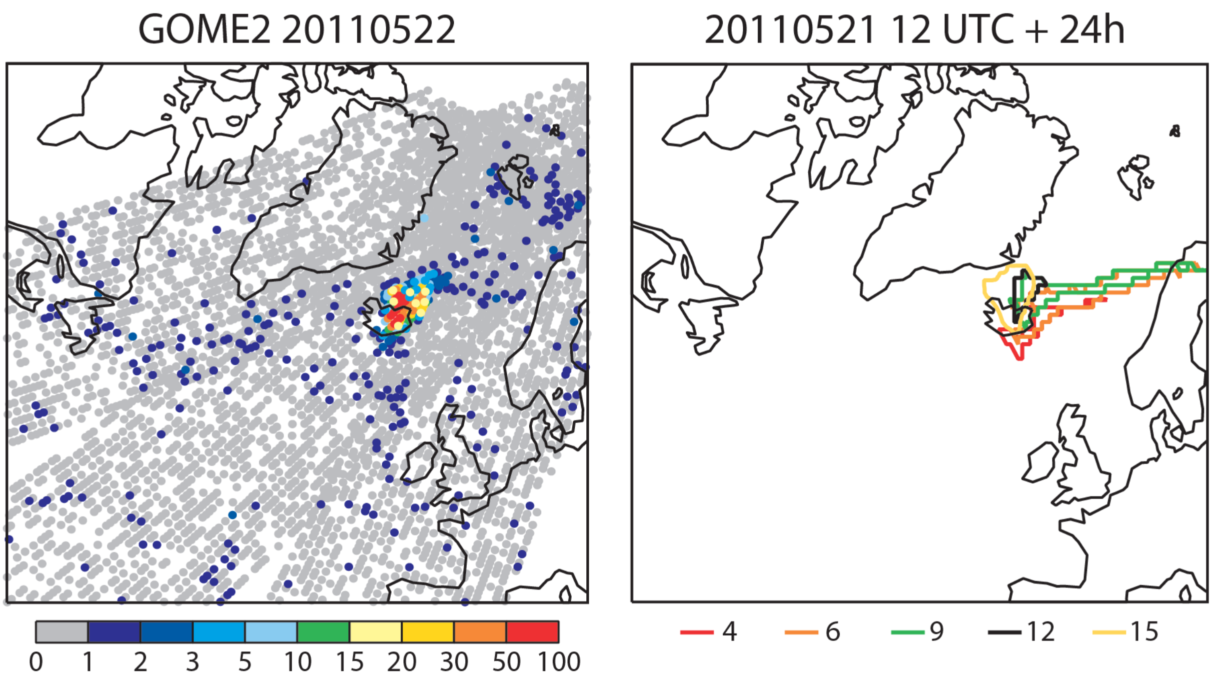


*Figure 6 Observed TCSO2 (GOME-2) on 22 May 2011 (left) (right) and the position of test tracer plumes released at 4, 6, 9 12 and 15 km 24 h before.*

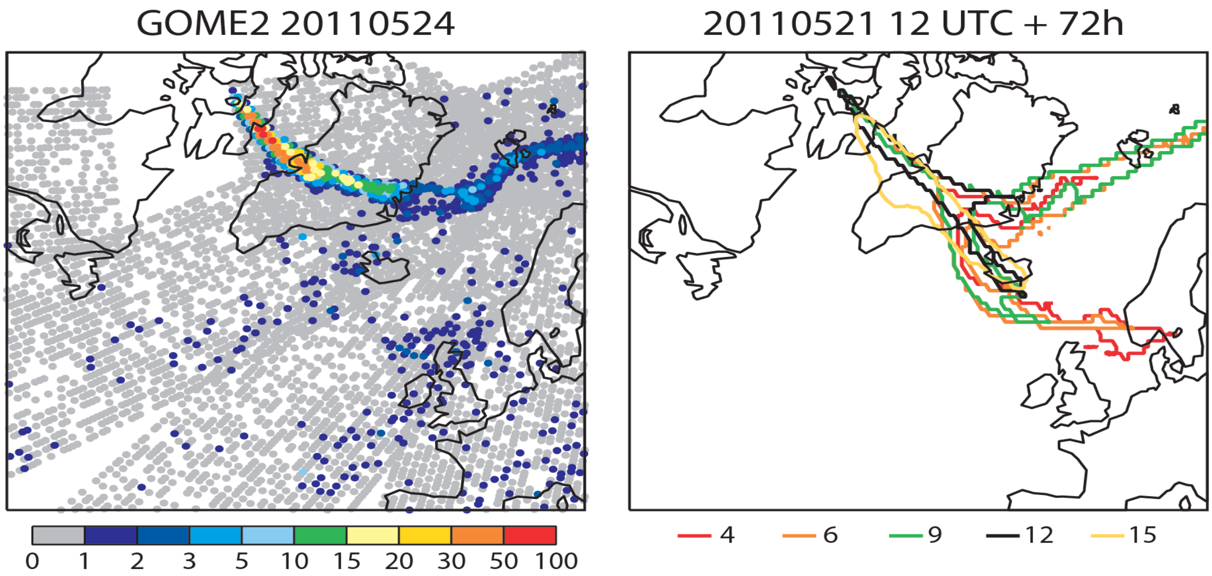


*Figure 7 Observed TCSO2 (GOME-2) on 24 May 2011 (left) and the position of tracer plumes released at 4, 6, 9 12 and 15 km 72 h before.*

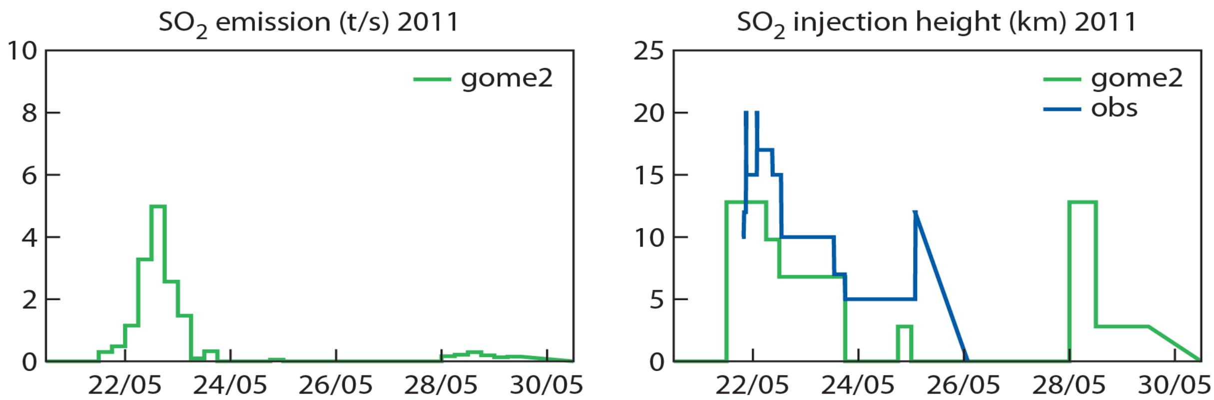


*Figure 8 $SO_2$ emission flux in t/s from Grímsvötn in May 2011 derived from GOME-2 satellite observations (left) and corresponding plume heights (right) and radar observations of the ash plume top (obs) .*

| Day | Hour | Injection Height [km] | $SO_2$ emission flux [t/s] |
|---|---|---|---|
| 20110521 | 12 | 12 | 0.301302 |
| 20110521 | 18 | 12 | 0.486341 |
| 20110522 | 0 | 12 | 1.1495 |
| 20110522 | 6 | 9 | 3.27751 |
| 20110522 | 12 | 6 | 4.98066 |
| 20110522 | 18 | 6 | 2.56435 |
| 20110523 | 0 | 6 | 1.46641 |
| 20110523 | 6 | 6 | 0.098054 |
| 20110523 | 12 | 6 | 0.323454 |
| 20110523 | 18 | - | 0 |

*Table 2 $SO_2$ emission flux in t/s and the injection height above orography in km from Grímsvötn in May 2011 estimated from GOME-2 observations.*

### 5.3 Estimate for Eyjafjallajökull in May 2010

An overview of the meteorological situation in May 2010 is given in *Petersen et al.* [*2010, 2012*]. Until the middle of May 2010, there was generally little wind shear in the troposphere and the $SO_2$ plume was mostly located south of Iceland. The wind direction changed about 10 days later into a more northerly direction. Flow patterns at different altitudes for the two periods and the observed $SO_2$ plume on 6 May in Figure 9.

Figure 10 shows the source strength and the plume height estimate based on the gridded satellite observations in May 2010. Table 3 contains the numerical data of the emission parameter estimate. In the considered period the emission varied between 0.2 and 0.6 t/s. The highest emission occurred between 6 and 7 and on 11 May. No emissions were found after 23 May. Because of the lack of wind shear the height estimates were more ambiguous than the estimates for Grímsvötn. The overlap of the test plumes with the observations did differ little for injection heights in the range of 4-9 km which led to a pronounced variability of the estimated plume height. The radar observations show most of the time plumes top heights of 5 km from 1-23 May while plume heights up to 10 km were observed on 5-6 May, and up to 7 km from the 13-17 May. *Rix et al.* [*2012*] report a retrieved plume height of 8-13 km for 5 May 2010. The plume estimate based on GOME-2 captured some of this variability but remained mostly at around 2-4 km.

The plume parameter estimates based on OMI and SCIAMACHY resulted in a similar range of the emission flux between 0.1 and 0.5 t/s until 23 May, but there were considerable differences in the day to day variability. Likewise, the injection height estimates showed some similar features during the times of increased observed values, but there was also a large amount of disagreement in the day-to-day variability of the actual height.

The amount of emitted $SO_2$ from 1 May until the end of the eruption was 0.14, 0.13 and 0.25 Tg based on OMI, SCIAMACHY and GOME-2 data, respectively. The GOME-2 estimate for the period from 14-30 April 2010 of 0.01 Tg demonstrated that the first period of the eruption did not significantly contribute to the total $SO_2$ burden. In summary, the $SO_2$ amount emitted during the 40 days of the Eyjafjallajökull eruption over 40 was about 80 % of the emissions of Grímsvötn emitted over 2.5 days.

The estimate of the emissions based on IASI retrievals by *Heard et al.* [*2012*] differs from our estimate based on UV-VIS observations. The IASI based estimate is mostly lower in the period from 5-12 May with average values around 0.1 t/s but much higher in the period from 13-18 May, when the IASIS emission rates are in the range of 0.6 to 1.0 t/s. The mass of emitted $SO_2$ from both volcanoes was smaller than that of other recent eruptions, e.g. Sarychev: 1.2 Tg [*Haywood et al., 2010*] and Mt. Kasatochi: 1.5 Tg [*Karagulian et al., 2010*]. *Schumann et al.* [*2011*] had roughly estimated the Eyjafjallajökull emissions of the order of 1Tg based on flight observations.

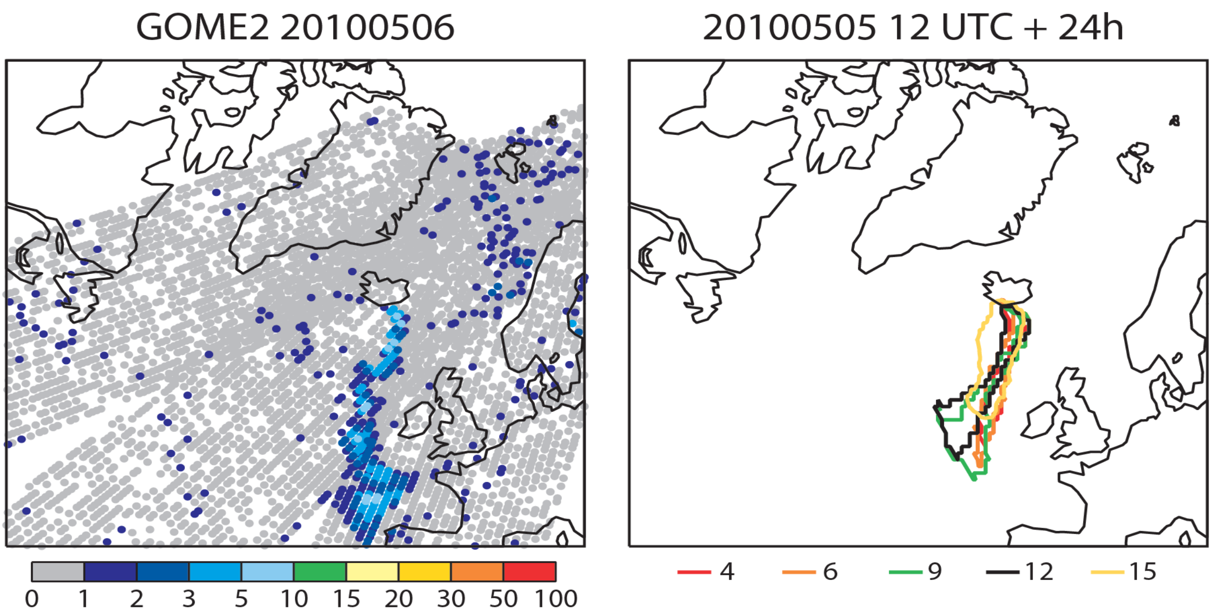


*Figure 9 Observed TCSO2 (GOME-2) on 6 May 2010 (left) and the position of tracer plume (right) released 24 h before at 3 at 4, 6, 9 12 and 15 km.*

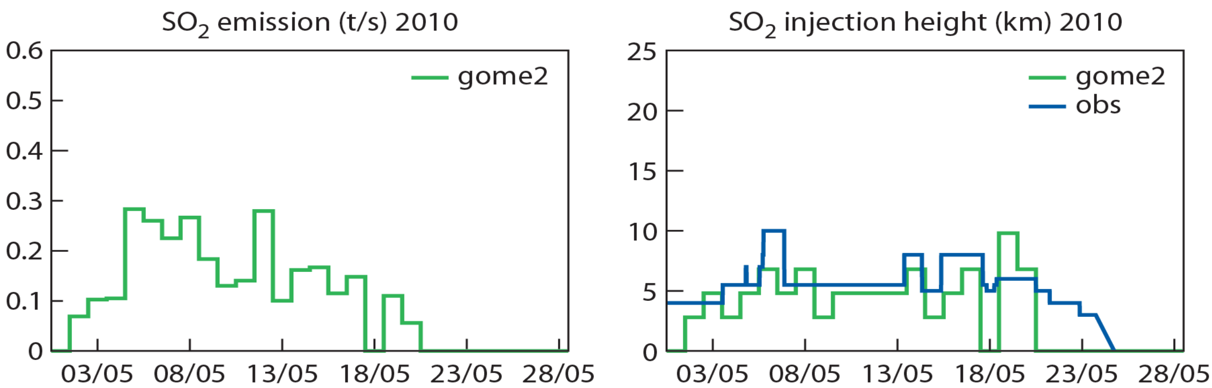


*Figure 10 $SO_2$ emission flux in t/s from Eyjafjallajökull in May 2010 derived from GOME-2 satellite observations (left) and corresponding plume heights (right) and radar observations of the ash plume top (obs)*

| Day | Hour | Injection Height [km] | $SO_2$ emission flux [t/s] |
|---|---|---|---|
| 20100501 | 12 | 2 | 0.068961 |
| 20100502 | 12 | 4 | 0.102665 |
| 20100503 | 12 | 2 | 0.104959 |
| 20100504 | 12 | 4 | 0.283181 |
| 20100505 | 12 | 6 | 0.259907 |
| 20100506 | 12 | 4 | 0.225235 |
| 20100507 | 12 | 6 | 0.266419 |
| 20100508 | 12 | 2 | 0.18346 |
| 20100509 | 12 | 4 | 0.130193 |
| 20100510 | 12 | 4 | 0.140489 |
| 20100511 | 12 | 4 | 0.2796 |

| | | | |
|---|---|---|---|
| 20100512 | 12 | 4 | 0.10032 |
| 20100513 | 12 | 6 | 0.161554 |
| 20100514 | 12 | 2 | 0.166971 |
| 20100515 | 12 | 4 | 0.115169 |
| 20100516 | 12 | 6 | 0.148133 |
| 20100517 | 12 | - | 0 |
| 20100518 | 12 | 9 | 0.109951 |
| 20100519 | 12 | 6 | 0.056098 |

*Table 3 $SO_2$ emission flux in t/s and the injection height above orography in km from Eyjafjallajökull in May 2010 estimated from GOME-2 observations*

# 6 Forecast and analysis of $SO_2$ plumes using GOME-2 observations

## 6.1 Error metric for volcanic plume analyses and forecasts

In the literature volcanic plume forecast are often only evaluated in a qualitative way based on maps. *Heard et al.* [*2012*] present a quantitative evaluation using hemispheric $SO_2$ averages, which tests the $SO_2$ budget but not the plume location. To quantify the plume forecast performance as well as the realism of the $SO_2$ analyses, an appropriate error measure needs to be defined. Standard error measures such as bias or root mean square error are less suitable because of the specific event-character of the plumes. We decided to use threshold based measures such as probability of detection (hit rate), which are also used for the verification of precipitation forecast [*WMO, 2008*]. In addition to these measures, which quantify the errors in the plume position, we also compared the number of pixels exceeding the threshold, which is a measure of the plume size regardless of the exact overlap. The following error measures were used:

- hits (both gridded observation and model/analysis exceed threshold)
- plume size (number of gridded observation or model/analyses exceeding threshold)

We used TCSO2 thresholds appropriate for the different plume characteristics in 2010 (2 and 5 DU) and 2011 (5 and 20 DU). To show the number of observed grid points exceeding the threshold, which were not predicted (missed), we show the number of gridded observation exceeding the threshold together with the hits. The number of false alarms, i.e. the model exceeds the threshold but the gridded observations do not, can be inferred from the difference between the model plume size and the hits.

Nevertheless, it remains difficult to account for the fact that the observed and the modelled plume do not always overlap but are actually very close to each other. Therefore the visual inspection of the observed and modelled plumes remains important.

It is good practice to evaluate the analyses with independent data, i.e. data which were not assimilated. However, the comparison with OMI and SCIAMACHY was not considered to be appropriate because of the biases and lower coverage of these data sets. Likewise, no sufficient in-situ data suited for an evaluation were available. Therefore forecasts as well as the analyses were only evaluated against the gridded GOME-2 TCSO2 retrievals (see section 2). The evaluation of the $SO_2$ analyses is a test to what extent the analyses resemble the assimilated observations.

## 6.2 Description of forecast runs

The GOME-2 data had the best spatial coverage of the three considered satellite instruments (see Figure 2). The experiments with the assimilation of the SCIAMACHY and OMI data were less successful than the assimilation of GOME-2 data. Therefore in this paper we only present forecasts based on GOME-2 observations.

All forecasts were carried out with the IFS at a T511 resolution using the model settings described in Section 4.1. 5 day forecasts were started at 12 UTC on several days. The forecast start at 12 UTC was chosen because only the 12 UTC analyses made use of the day–time satellite observations. The meteorological initial conditions for all forecasts were taken from the ECMWF operational model with a resolution of T799 in May 2010 and T1279 in May 2011.

Three main sets of forecasts were made, which differ in the choice of emissions and the initial conditions:

- Forecast with $SO_2$ source parameter derived only (EMI)
- Forecast with $SO_2$ analysis as initial conditions only and no $SO_2$ source term (INI)
- Forecast with $SO_2$ analysis as initial conditions and estimated $SO_2$ source terms (INIEMI)

The initial $SO_2$ conditions for the EMI runs were taken from the previous forecast, whereas for INI and INIEMI the $SO_2$ analysis was used. The $SO_2$ emission flux estimate was used in the runs EMI and INIEMI. The estimate of the injection height and the plume height was used in all three forecast runs.

## 6.3 Evaluation for Grímsvötn in May 2011

The temporal development of the plume with respect to 5 and 20 DU was well captured by the INI, EMI and INIEMI 24h forecast (see Figure 11). About 50-80% of the observations were correctly forecast (hits) but the plumes tended to exaggerate the plume area by up to 100%. Overall the INIEMI forecasts showed the best performance both during the eruption and up to 10 days after the eruption. An example of the observed and forecast plumes during (23 May) and after the eruption (26 May) is shown in Figure 13. Without emissions present after the eruption, the forecast of INI and INIEMI were very similar. However, the initialisation alone (INI) led to poorer forecasts compared to the forecast using a source term (EMI and INIEMI) during the eruption.

The model using the source term only (EMI) did not manage to simulate the fate of the plume with respect to the high observed maximum values (see Figure 3) over a period of 10 days. The movement of the $SO_2$ plume over Greenland and its return to Iceland south of Greenland was a characteristic feature of this eruption and was well observed by GOME-2, OMI and SCIAMACHY. The re-circulated plume still maintained TCSO2 of up 30 DU when it crossed Iceland 5 days after the eruption.

The plume shapes of the EMI forecasts were more confined and more similar to the observations than the initialised forecasts (INI and INIEMI) up to 5 days after the eruption. However, the forecast plume maxima were too low and a distinct plume ceased to exist in the EMI forecasts after 28 May. This does not seem to be a consequence of an underestimation of the emissions source term because the EMI forecast tended to overestimate the plume strength during the eruption. The lifetime assumption used for the forecasts (10 days) could be a potential explanation for this behaviour but test runs with a lifetime of 20 days did not fundamentally solve the problem. We suspect that excessive numerical diffusion of the IFS advections scheme is main reason for the over-dispersive model results and more tests will be carried out to investigate this further.

Figure 12 shows the hit and the plume area for INI and EMI forecasts with different forecast lengths of 24, 48 and 72 hours as well as for the analysis (0 h). The EMI forecasts showed only little changes in forecast performance for different lead times. Since we always used the full information of the source term in the EMI forecasts the change was caused by the meteorological forecast errors, which were of minor importance compared to the uncertainties of the plume characteristics. The INI forecasts at longer lead times were significantly poorer than the 24h forecast. This was due to the fact that without source information no useful forecast can be made from before the eruption. The decreased performance after the eruption could have been caused by the same excessive dispersion already noted for the 24 h EMI forecasts.

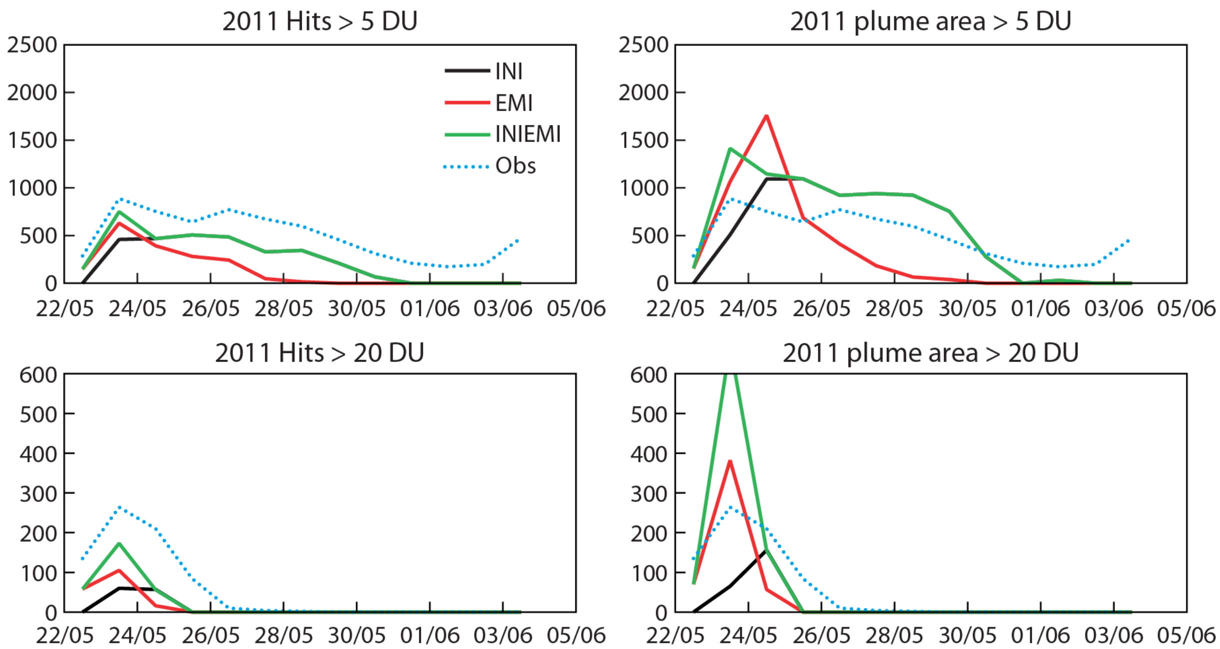


*Figure 11 Hits (left) and plume area (right) for the threshold 5 DU (top) and 20 DU (bottom) in May 2011 for the 24h forecasts of INI, EMI and INIEM. Also show is the number of gridded observations (Obs) above the threshold*

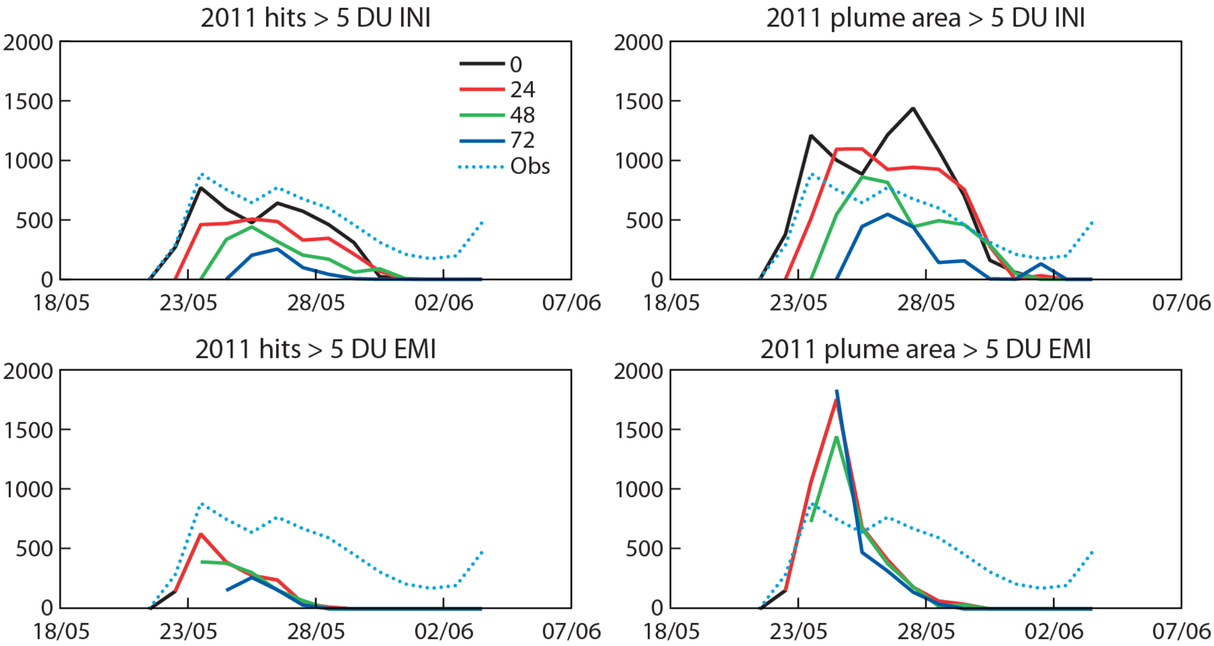


Figure 12 Hits (left) and plume area (right) of analysis (0) and forecasts over 24, 48 and 72 hours from INI (top) and EMI (bottom) for the threshold 2 DU in May 2011. Also shown is the number of gridded observations (Obs) above the threshold.

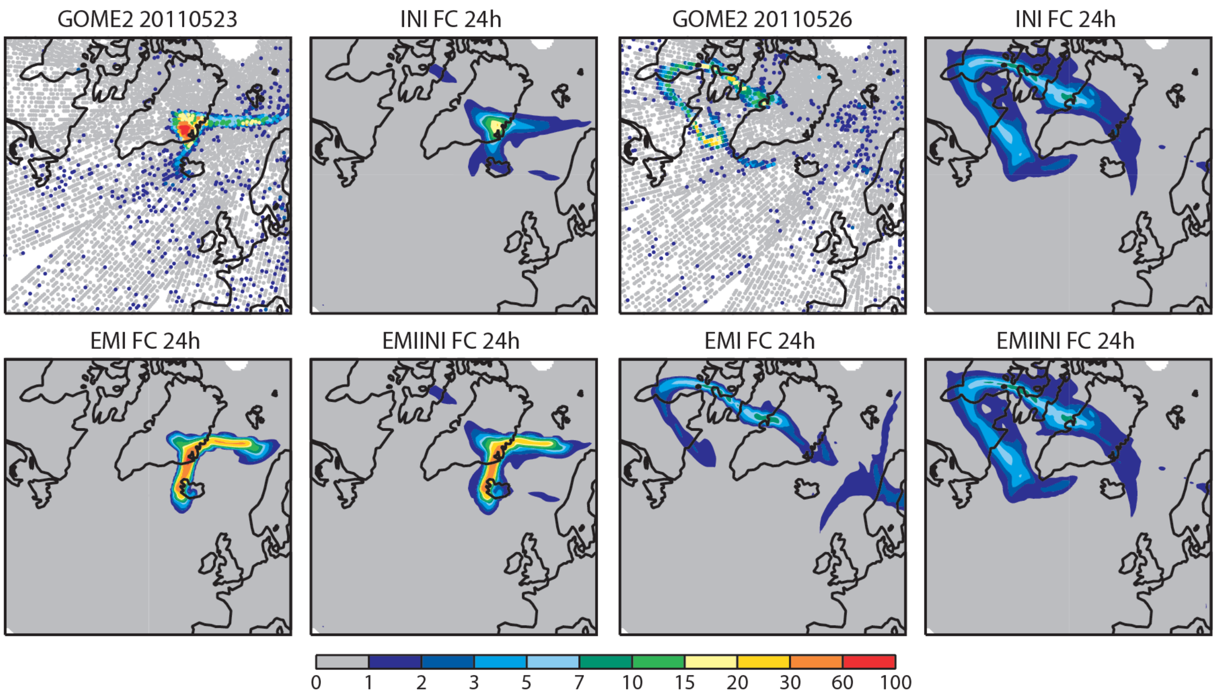


Figure 13 GOME-2 observations and 24h forecasts from INI, EMI and INIEM for the 23 May (left) and 26 May (right) 2011.

## 6.4 Evaluation for Eyjafjallajökull in May 2010

Hits and plume areas above the thresholds 2 and 5 DU (see section 6.1) of the 24 h forecast (INI, EMI, INIEMI) and the analysis (ANA) are shown in Figure 14 and Figure 15 for the Eyjafjallajökull eruption. Figure 16 shows as an example the GOME-2 TCSO2 retrievals for 8 and 12 May 2010.

The analyses capture correctly the temporal development of the TCSO2 values for different thresholds. 50-90% of the gridded observations are correctly forecast (hit) but the analyses tend to exaggerate the plume size.

TCSO2 values exceeding 2 DU (Figure 14) were observed from 5-13 May and to a smaller extent around 16 May. The same variability of the plume extent was reproduced by the all forecasts, with INIEMI and EMI showing the best match with the observations. A fraction of 20-30% percent were hits with respect to the exact location. However, the visual inspection of the observed and modeled plumes (see Figure 16) reveals a reasonable resemblance of the plume shape and location. The INI forecasts, which have no emission source term lack the plume parts emitted during the forecast period. In contrast, the EMI forecasts tend to underestimate the strength of the older plumes, which may be caused by errors in the emission estimate, the assumption about the lifetime or exaggerated dispersion by the IFS model.

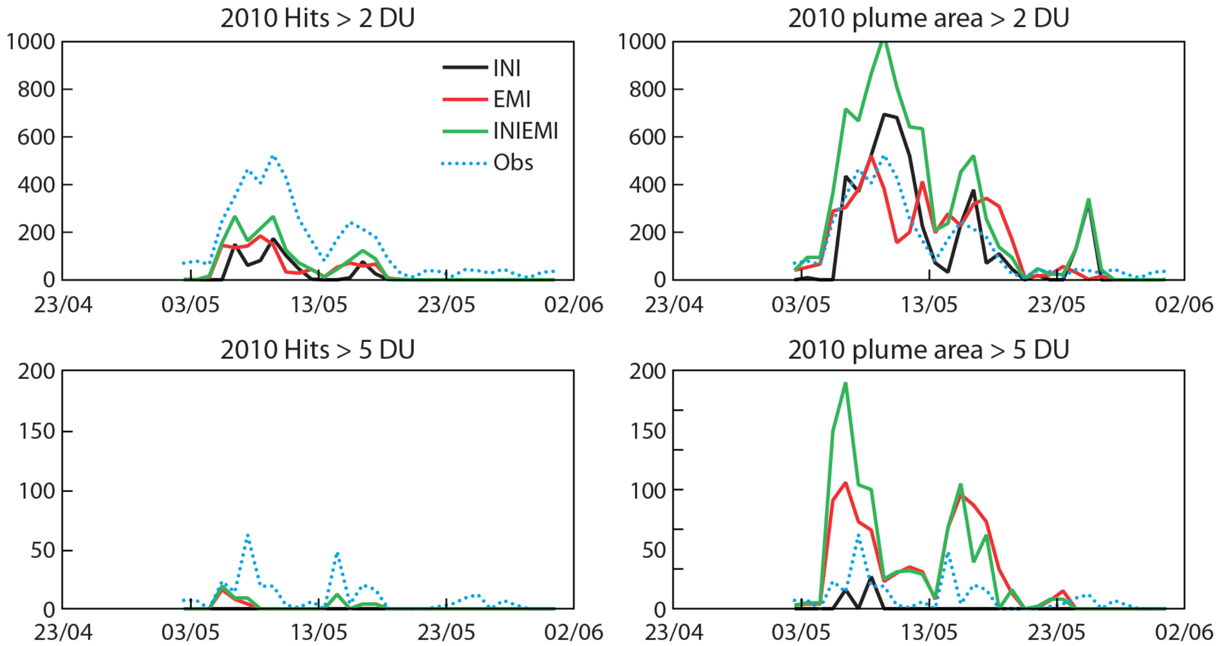


*Figure 14 Hits (left) and plume area (right) for the threshold 2 DU (top) and 5 DU (bottom) in May 2010 for the 24h forecast INI, EMI and INIEM Obs is the number of grid point of the gridded observations (Obs) above the threshold.*

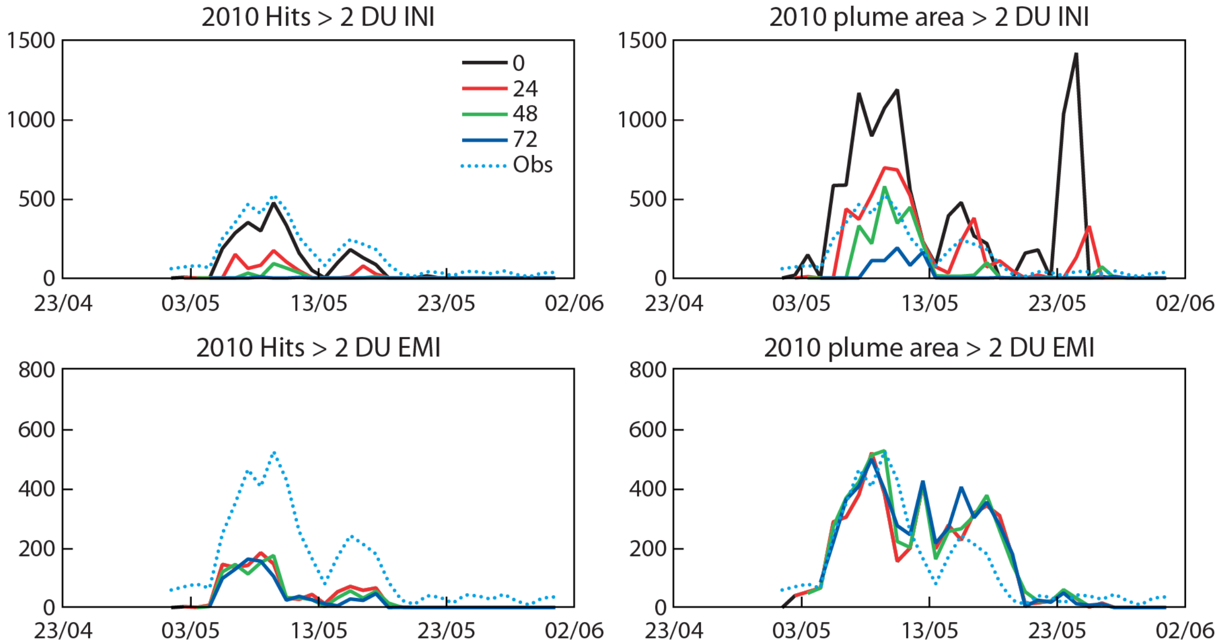


*Figure 15 Hits (left) and plume area (right) of analysis (0) and the INI forecast over 24, 48 and 72 hours for the threshold 2 DU in May 2010. Obs is the number of grid point of the gridded observations (Obs) above the threshold*

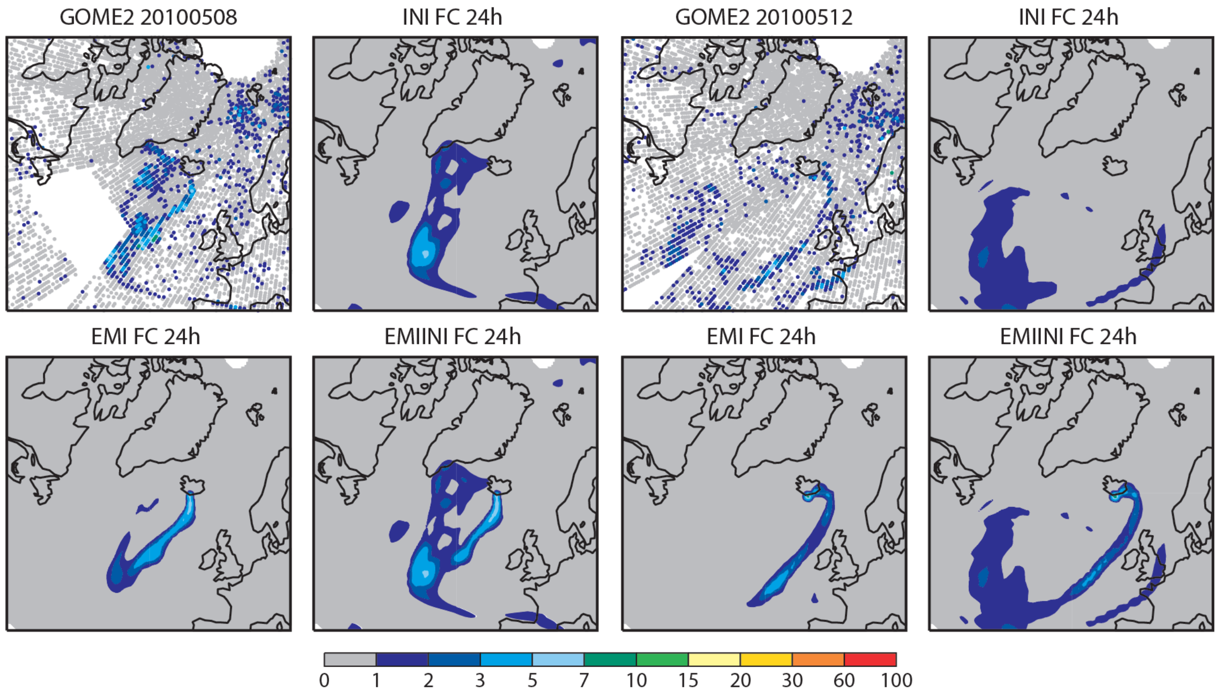


*Figure 16 GOME-2 observations and the 24h forecasts INI, EMI and INIEM for 8 (left) and the 12 May (right) 2010.*

# 7 Discussion

The simulation and the assimilation of the studied volcanic $SO_2$ plumes have large uncertainties. An important piece of information for the simulation is the injection height of the plume and for the assimilation the height of the entire plume. Although the top height of the ash plume was observed during both events, it cannot be assumed that this corresponds to the injection height for $SO_2$. Further, injection height observations are not available for all volcanoes worldwide. Therefore, we saw the need to develop a method, which estimates source strength and source height from global satellite observations. The occurrence of vertical wind shear, and its correct representation by the meteorological model was crucial to extract information about the plume height from the TCSO2 retrievals. The presented method assumed that the injection occurs in only one of the prescribed height intervals. There was ambiguity in the automated choice of the plume that matches best the observations with respect to shape, in particular for the 2010 case with little wind shear. On the other hand, a lack of vertical wind shear, would not lead to large errors in the horizontal position of the plume, if the injection height estimate was incorrect. The satellite observations used in this study lacked information about the plume height although progress has been made in the past to extract the injection as part of the retrieval process [*Rix et al., 2012* and *Yang et al., 2009*].

Good data coverage is important for our method to work. For successful source-term estimates as well as the assimilation of the data, the $SO_2$ data have to cover the complete extent of the plume as well as a sufficient area outside the plume. In our study only the GOME-2 data fulfilled this criterion. A limitation of all UV-VIS satellite observations from polar orbiting platforms is their availability only once a day, which makes it difficult to capture the pronounced variability (see Figure 8 and Figure 10 for the injection height) of the volcanic emissions at a time scale of hours. Estimates of the $SO_2$ lifetime and the emission strength depend further on the quality of the satellite retrievals for the determination of the total $SO_2$ burden. From the day-to-day variability of the observed total burdens over a larger area in 2009, i.e. a period without an eruption, we deduced an uncertainty equivalent to a source / sink term of about +/- 0.3 t/s. This value is of the same magnitude as the derived emissions for the Eyjafjallajökull eruption in May 2010. With our approach to estimate the source strength (see section 5.1), we reduced this uncertainty by considering only the area covered by a plume simulation. Further limitations for the correct determination of the burden of the $SO_2$ emissions estimate were non-linear biases such as saturation for high values, a constant offset, or detection limits in the low range. The OMI retrievals had higher maximum values than the retrieval from the other instruments, which cannot be explained by the smaller OMI pixel size alone. The differences in the high values and the background can hamper the correct estimation of the burden of highly concentrated or more diluted plumes. For example, we found larger differences in the estimation of the lifetime for 2011 based on OMI and GOME-2 data (see section 4.2). The evaluation of $SO_2$ satellite retrievals should therefore consider the temporal consistency of the observation with respect to the total burden. For example, *Haywood et al.* [*2010*] report a strong increase of the estimated $SO_2$ lifetime based on IASI data for the Sarychev eruption in 2008 if the detection limit is taken into account.

The correct simulation of the plume is a challenge for the meteorological model and its advection scheme. In particular the fate of the plume in 2011 after the eruption, as noted by [*Kerminen et al. 2011*], is difficult to simulate. In this paper we did not discuss in detail aspects of transport and chemical modelling although they play a large role for the correct simulation. The good forecast performance of the plume shape of the 24, 48 and 72 hours EMI forecast leads to the conclusion that the IFS produced a realistic meteorological forecast over the whole period. However, the IFS model seems to the greatly exaggerate the dispersion of the modelled plume, which led to a much stronger decrease in the modelled plume maxima than in the observations, in particular for 2011.

We applied a $SO_2$ lifetime of 10 days based on the estimate of the OMI and GOME-2 data, which is about the same size as the lifetime estimate by *Krotkov et al.* [*2010*] for the 2008 Kasatochi eruption. Test runs with a 20 day $SO_2$ lifetime did not solve the problem of the IFS model failing to maintain the high TCSO2 values after the 2011 eruption.

The presented procedure can be applied in near-real time (NRT) to provide emission and injection height estimates as well as forecasts of $SO_2$ for volcanic eruptions. The satellite observations for a day can be used to estimate the emission and height term for the previous 24 hours (EMI) and can be assimilated to initialise the forecast (INI and INEMI). However emission data will not be known for the forecast run, and assumptions about the future emissions have to be made. One potential application would be to have two forecasts runs starting form initial conditions based on data assimilation, one without emissions (as in the INI simulation) and one with the constant continuation of the last observation based estimate to derive possible scenarios. The former would have been more appropriate for the 2011 case and the latter for 2010 case. It should be noted that the INI runs also require information about the plume height during the data assimilation procedure (see section 3.2). The MACC NRT forecasting and data assimilation system (http://www.gmes-atmosphere.eu//) is using an implementation of the INI scenario with an ad-hoc assumption of an injection height of 5 km to provide NRT $SO_2$ forecasts in the event of volcanic eruptions.

# 8 Summary

We forecast the $SO_2$ plumes of the eruption of Grímsvötn in May 2011 and during the second phase of the Eyjafjallajökull eruption in May 2010. $SO_2$ was released from Eyjafjallajökull until 23 May with two more intense periods around 5-10 and 13-18 May 2010. The $SO_2$ plume was predominantly transported in a southward direction and was co-located with the ash plume. The 2011 eruption of Grímsvötn was shorter but more intense and released larger amounts of $SO_2$ over the period from the 21-23 May 2011. Large vertical wind shear led to a separation of the $SO_2$ and the ash plume. Most of the $SO_2$ was transported in a well-confined plume north-westwards to Newfoundland before it returned to Iceland on 28 May, after which it moved as a more dispersed plume further towards Northern Siberia.

We inter-compared satellite retrievals of the TCSO2 by GOME-2, OMI and SCIAMACHY with respect to the median, P99 and total burdens for estimates of the lifetime. The position of the observed plumes agreed well between the instruments. The OMI observations gave the highest observed values, even after taking into account the influence of the different pixel sizes of the instruments. The GOME-2 data had the highest median values. The derived $SO_2$ lifetime was the longest in 2011 for the GOME-2 data. The GOME-2 satellite observations had the most complete spatial coverage of all instruments, which is why only GOME-2 data were used to facilitate and evaluate the $SO_2$ forecasts.

We presented an approach to estimate the plume injection height and the $SO_2$ emission source term by considering satellite TCSO2 retrievals (see Figure 8 and Figure 10). The applied methodology led to emission estimates of 0.13-0.25 Tg over 20 days in May 2010 and 0.32-0.39 Tg over 36 hours in 2011. We used the amount of overlap of the observed plume with test tracer plumes emitted at different levels to determine the injection height. The estimate of the mass flux was based on the area covered by the test plume with the most likely injection height. The estimated injection height compared well with observed plume top height of the ash plume in 2011, and reasonably well with the observations in 2010 because of the less strong vertical wind shear. Although of the same order of magnitude, our GOME-2 based estimate of the $SO_2$ flux was higher in the period from 5-11 May 2010 and lower during the second peak from 13-18 May 2010 than an IASI based estimate by *Heard et al.* [*2012*].

As well as using TCSO2 satellite retrievals to estimate the source term, we also assimilated the GOME-2 TCSO2 retrievals to make the simulation more realistic by correcting the initial conditions. We used the MACC data assimilation system for atmospheric composition to produce 3-dimensional $SO_2$ analyses. The MACC system is an extension of ECMWF's IFS. Since the assimilated TCSO2 retrievals did not contain information about the plume height we used the averaged injection height estimates to place the $SO_2$ plumes at an appropriate vertical level as part of the data assimilation procedure. The TCSO2 analyses agreed very well with the assimilated observations but had a tendency to exaggerate the plume extent. This was probably caused by the predefined specification of the horizontal background error correlation.

We carried out five-day forecasts for both May 2010 and May 2011 starting from 12 UTC with three different configurations: the EMI forecasts used the estimated source terms, the INI forecasts were initialised with $SO_2$ analyses only, and the INIEMI forecasts were initialised with $SO_2$ analyses and used the source terms . The IFS was used for the forecasts and the assimilation at a resolution of T511, which corresponds to a grid box size of about 40 x 40 km. The forecasts were evaluated with respect to the exceedance of thresholds of 2, 5 and 20 DU as well as the plume size for these thresholds. Overall, the INIEMI forecasts were of the highest accuracy. The use of a source term was beneficial during the eruption and in the vicinity of the source. The initialisation (in INI and INIEMI) had the largest benefit after the eruption since it could compensate for inability of the IFS model to maintain the high TCSO2 values of the observed plume.

A NRT implementation of a volcanic $SO_2$ plume forecasting system can be run in the INI setup without further modifications. NRT estimates of the emissions flux and the injection height can be made up to the time of the TCSO2 retrievals available at the forecast start. However, scenarios need to be defined about the continuation of the emission parameters during the forecast length.

## Acknowledgements

The study has been carried out as part of the MACCII project, which is funded by the European Commission under the EU Seventh Research Framework Programme. Martin Suttie (ECMWF) is acknowledged for processing of the satellite data. We thank Claire Whitman (UK met-office) providing the radar observation of the plume height and Nickolay Krotkov (NASA GSFC) for advice on the OMI data. The OMI data have been produced by NASA-GSFC, the GOME-2 data by DLR and the SCIAMACHY data by BIRA.

## References

Benedetti, A., J. W. Kaiser, J-J. Morcrette, R. Eresmaa and S. Lu (2011), Simulations of volcanic plumes with the ECMWF/MACC aerosol system, December 2011, *ECMWF Technical Memorandum, 653*, http://www.ecmwf.int/publications/library/do/references/list/14.

Bovensmann, H., J. P. Burrows, M. Buchwitz, J. Frerick, S. Noël, V. V. Rozanov, K. V. Chance, A. P. H. Goede (1998), SCIAMACHY – Mission objectives and measurement modes. *J. Atmos. Sci*., Vol. 56, pp. 127 – 150.

Bukowiecki, N., Zieger, P., Weingartner, E., Jurányi, Z., Gysel, M., Neininger, B., Schneider, B., Hueglin, C., Ulrich, A., Wichser, A., Henne, S., Brunner, D., Kaegi, R., Schwikowski, M., Tobler, L., Wienhold, F. G., Engel, I., Buchmann, B., Peter, T., and Baltensperger, U. (2011), Ground-based and airborne in-situ measurements of the Eyjafjallajökull volcanic aerosol plume in Switzerland in spring 2010, *Atmos. Chem. Phys*., 11, 10011-10030, doi:10.5194/acp-11-10011-2011.

Carn, S. A., A. J. Krueger, S. Arellano, N. A. Krotkov, and K. Yang (2008), Daily monitoring of Ecuadorian volcanic degassing from space. *J. Volcanol. Geoth. Res*., Vol, 176(1), pp. 141-150, doi: 10.1016/j.jvolgeores.2008.01.029.

Carn, S. A., A. J. Krueger, N. A. Krotkov, K. Yang, and K. Evans (2009), Tracking volcanic sulfur dioxide clouds for aviation hazard mitigation. *Nat. Hazards*, Vol. 51(2), pp. 325-343, doi:10.1007/s11096-008-9228-4.

Clarisse, L., Coheur, P. F., Prata, A. J., Hurtmans, D., Razavi, A., Phulpin, T., Hadji-Lazaro, J., and Clerbaux, C., (2008), Tracking and quantifying volcanic SO$_2$ with IASI, the September 2007 eruption at Jebel at Tair, *Atmos. Chem. Phys*., 8, 7723-7734, doi:10.5194/acp-8-7723-2008.

Dacre, H.F., A. L. M. Grant, R. J. Hogan, S. E. Belcher, D. J. Thomson, B. Devenish, F. Marenco, M. C. Hort, J. M. Haywoood, A. Ansmann, I. Mattis, L. Clarisse (2011), Evaluating the structure and magnitude of the ash plume during the initial phase of the 2010 Eyjafjallajokull eruption using lidar observations and NAME simulations, *J. Geophys. Res*., 116, D00U03, doi:10.1029/2011JD015608.

Daley, R., (1991), *Atmospheric Data Analysis*. Cambridge Atmospheric and Space Science Series, Cambridge University Press. ISBN 0-521-38215-7, 457 pages.

Doeringer, D., A. Eldering, C. D. Boone, G. González Abad, and P. F. Bernath (2012), Observation of sulfate aerosols and $SO_2$ from the Sarychev volcanic eruption using data from the Atmospheric Chemistry Experiment (ACE), *J. Geophys. Res*., 117, D03203, doi:10.1029/2011JD016556.

Eckhardt, S., A. J. Prata, P. Seibert, K. Stebel, A. Stohl (2008), Estimation of the vertical profile of sulfur dioxide injection into the atmosphere by a volcanic eruption using satellite column measurements and inverse trajectory modelling, *Atmos. Chem. Phys*., 8, 3881-3897, doi:10.5194/acp-8-3881-2008.

Eisinger, M. and J.P. Burrows (1998), Tropospheric sulfur dioxide observed by the ERS-2 GOME instrument. *Geophys. Res. Lett*., Vol. 25, pp. 4177-4180.

Emeis, S., R. Forkel, W. Junkermann, K. Schäfer, H. Flentje, S. Gilge, W. Fricke, M. Wiegner, V. Freudenthaler, S. Groβ, L. Ries, F. Meinhardt, W. Birmili, C. Münkel, F. Obleitner, and P. Suppan (2009), Measurement and simulation of the 16/17 April 2010 Eyjafjallajökull volcanic ash layer dispersion in the northern Alpine region, *Atmos. Chem. Phys*., 11, 2689-2701.

Flemming, J., Inness, A., Flentje, H., Huijnen, V., Moinat, P., Schultz, M. G., and Stein, O. (2009), Coupling global chemistry transport models to ECMWF's integrated forecast system, *Geosci. Model Dev*., 2, 253-265.

Flemming, J., Inness, A., Jones, L., Eskes, H. J., Huijnen, V., Schultz, M. G., Stein, O., Cariolle, D., Kinnison, D., and Brasseur, G. (2011) , Forecasts and assimilation experiments of the Antarctic ozone hole 2008, *Atmos. Chem. Phys*., 11, 1961-1977, doi:10.5194/acp-11-1961-2011.

Fisher, M. (2004), Generalized frames on the sphere with application to background error covariance modelling, *in: Proceedings of the Seminar on resent developments in numerical methods for atmospheric and ocean modelling*, 6–10 September 2004, ECMWF, 87–101, available from ECMWF, Shinfield Park, Reading, Berkshire, RG2 9AX, UK.

Fisher, M., (2006), Wavelet 5 Jb – a new way to model the statistics of background errors, *ECMWF Newsletter*, 106, 23–28, available from ECMWF, Shinfield Park, Reading, Berkshire, RG2 9AX, UK.

Gudmundsson, M.T., R. Pedersen, K. Vogfjörd, B. Thorbjarnardottir, S. Jakobsdottir, M.J. Roberts (2010), Eruptions of Eyjafjallajökull Volcano, Iceland. *Eos*, Vol. 91, No. 21, pp. 190-191.

Haywood, J. M., et al. (2010), Observations of the eruption of the Sarychev volcano and simulations using the HadGEM2 climate mode, *J. Geophys. Res*., 115, D21212, doi:10.1029/2010JD014447.

Heard, I. P. C., A. J. Manning, J. M. Haywood, C. Witham, A. Redington, A. Jones, L. Clarisse, and A. Bourassa (2012), A comparison of atmospheric dispersion model predictions with observations of $SO_2$ and sulphate aerosol from volcanic eruptions, *J. Geophys. Res*., 117, D00U22, doi:10.1029/2011JD016791.

Heue, K.-P., C.A.M. Brenninkmeijer, A. K. Baker, A. Rauthe-Schöch, D. Walter, T. Wagner, C. Hörmann, H. Sihler, B. Dix, U. Frieß, U. Platt, B.G. Martinsson, P.F.J. van Velthoven, A. Zahn, R. Ebinghaus (2011), $SO_2$ and BrO observation in the plume of the Eyjafjallajökull volcano 2010: CARIBIC and GOME-2 retrievals. *Atmos. Chem. Phys*., Vol. 11, pp. 2973–2989.

Hollingsworth, A., Engelen, R.J., Textor, C., Benedetti, A., Boucher, O., Chevallier, F., Dethof, A., Elbern, H., Eskes,H., Flemming, J., Granier, C., Kaiser, J.W., Morcrette, J.-J., Rayner, P., Peuch, V.H., Rouil, L., Schultz, M.G., Simmons, A.J and The GEMS Consortium, (2008),Towards a Monitoring and Forecasting System For Atmospheric Composition: The GEMS Project,. *Bull. Amer. Meteor. Soc*., 89, 1147-1164.

Hughes, E. J., L. C. Sparling, S. A. Carn, and A. J. Krueger (2012), Using horizontal transport characteristics to infer an emission height time series of volcanic $SO_2$, *J. Geophys. Res*., 117, D18307, doi:10.1029/2012JD017957.

Inness, A., Baier, F., Benedetti, A., Bouarar, I., Chabrillat, S., Clark, H., Clerbaux, C., Coheur, P., Engelen, R. J., Errera, Q., Flemming, J., George, M., Granier, C., Hadji-Lazaro, J., Huijnen, V., Hurtmans, D., Jones, L., Kaiser, J. W., Kapsomenakis, J., Lefever, K., Leitão, J., Razinger, M., Richter, A., Schultz, M. G., Simmons, A. J., Suttie, M., Stein, O., Thépaut, J.-N., Thouret, V., Vrekoussis, M., Zerefos, C., and the MACC team, (2012), The MACC reanalysis: an 8-yr data set of atmospheric composition*, Atmos. Chem. Phys. Discuss*., 12, 31247-31347, doi:10.5194/acpd-12-31247-2012.

Kerminen, V.-M., Niemi, J. V., Timonen, H., Aurela, M., Frey, A., Carbone, S., Saarikoski, S., Teinilä, K., Hakkarainen, J., Tamminen, J., Vira, J., Prank, M., Sofiev, M., and Hillamo, R. (2011), Characterization of a volcanic ash episode in southern Finland caused by the Grímsvötn eruption in Iceland in May 2011*, Atmos. Chem. Phys*., 11, 12227-12239, doi:10.5194/acp-11-12227-2011.

Kristiansen, N.I., A. Stohl, A.J. Prata, A. Richter, S. Eckhardt, P. Seibert,A. Hoffmann, C. Ritter, L. Bitar, T.J. Duck, K. Stebel (2010). Remote sensing and inverse transport modeling of the Kasatochi eruption sulfur dioxide cloud*. J. Geophys. Res*., Vol. 115, D00L16, doi:10.1029/2009JD013286.

Krotkov, N.A., M. R. Schoeberl, G. A. Morris, S. Carn, and K. Yang (2010). Dispersion and lifetime of the $SO_2$ cloud from the August 2008 Kasatochi eruption*, J. Geophys. Res*, 15(D00L20), 10.1029/2010JD013984.

Krueger, A. J., L. S. Walter, P. K. Bhartia, C. C. Schnetzler, N. A. Krotkov, I. Sprod, and G. Bluth (1995), Volcanic sulfur dioxide measurements from the Total Ozone Mapping Spectrometer (TOMS) instruments*, J. Geophys. Res*., 100, 14,057–14,076, doi:10.1029/95JD01222.

Lee, C., Martin, R. V., van Donkelaar, A., O'Byrne, G., Krotkov, N., Richter, A., Huey, G., Holloways, J. S., (2009), Retrieval of vertical columns of sulfur dioxide from SCIAMACHY and OMI: Air mass factor algorithm development and validation, *J. Geophys. Res*., 114, D22303, doi:10.1029/2009JD012123.

Lee, C., Richter, A., Weber, M., Burrows, J. P. (2008), $SO_2$ retrieval from SCIAMACHY using the weighting function DOAS (WFDOAS) technique: comparison with standard DOAS retrieval, *Atmos. Chem. Phys*., 8, 6137-6145.

Levelt, P.F., G.H.J. van den Oord, M.R. Dobber, A, Malkki, H. Visser, J. de Vries, P. Stammes, J. Lundell, H. Saari (2006). The Ozone Monitoring Instrument, *IEEE Trans. Geosci. Remote Sens*., Vol. 44, No. 5, pp. 1093-1101.

Mahfouf J.-F. and F. Rabier, (2000), The ECMWF operational implementation of four-dimensional variational assimilation.II, Experimental results with improved physics. *Q. J. R. Met. Soc.,* Vol. 126, No. 564, pp 1171.

Mastin et al. (2009), A multidisciplinary effort to assign realistic source parameters to models of volcanic ash-cloud transport and dispersion during eruptions. *J. Volcanology and Geothermal Research* 186, 10-21, 2009.

Morcrette, J.-J., et al. (2009), Aerosol analysis and forecast in the European Centre for Medium-Range Weather Forecasts Integrated Forecast System: Forward modeling, *J. Geophys. Res*., 114, D06206, doi:10.1029/2008JD011235.

Newhall, C.G., and Self, S., (1982), The volcanic explosivity index (VEI): An estimate of explosive magnitude for historical volcanism, *Journal of Geophysical Research*, v. 87, p. 1231-1238.

Petersen, G.N. (2010), A short meteorological overview of the Eyjafjallajökull eruption 14 April–23 May 2010. *Weather,* August 2010, Vol. 65, No. 8.

Petersen, G. N., H. Bjornsson, and P. Arason (2012), The impact of the atmosphere on the Eyjafjallajökull 2010 eruption plume, *J. Geophys. Res*., 117, D00U07, doi:10.1029/2011JD016762.

Platt, U. (1994), Differential optical absorption spectroscopy (DOAS). In: Air Monitoring by Spectroscopic Techniques. *Chem. Anal.* Ser., Vol. 127, pp. 27-84, John Wiley, New York.

Parrish, D. F. and Derber, J. C. (1992), The national meteorological center's spectral statistical interpolation analysis scheme, *Mon. Weather Rev*., 120, 1747–1763.

Prata, A. J., and C. Bernardo (2007), Retrieval of volcanic $SO_2$ column abundance from Atmospheric Infrared Sounder data, *J. Geophys. Res*., 112, D20204, doi:10.1029/2006JD007955.

Prata, J. (2008), Satellite detection of hazardous volcanic ash clouds and the risk to global air traffic. *Nat. Hazards*, doi:10.1007/s11096-008-9273-z.

Rix, M., P. Valks, N. Hao, J. van Geffen, C. Clerbaux, L. Clarisse, P.-F. Coheur, D. Loyola, T. Erbertseder, W. Zimmer, S. Emmadi (2009), Satellite Monitoring of Volcanic Sulfur Dioxide Emissions for Early Warning of Volcanic Hazards. *IEEE Journal of Selected Topics in Applied Earth Observations and Remote Sensing*, Vol. 2, No. 3, pp. 196-206.

Rix, M., P. Valks, N. Hao, D. Loyola, H. Schlager, H. Huntrieser, J. Flemming, U. Koehler, U. Schumann, and A. Inness (2012), Volcanic $SO_2$, BrO and plume height estimations using GOME-2 satellite measurements during the eruption of Eyjafjallajökull in May 2010, *J. Geophys. Res*., 117, D00U19, doi:10.1029/2011JD016718.

Schumann, U., Weinzierl, B., Reitebuch, O., Schlager, H., Minikin, A., Forster, C., Baumann, R., Sailer, T., Graf, K., Mannstein, H., Voigt, C., Rahm, S., Simmet, R., Scheibe, M., Lichtenstern, M., Stock, P., Rüba, H., Schäuble, D., Tafferner, A., Rautenhaus, M., Gerz, T., Ziereis, H., Krautstrunk, M., Mallaun, C., Gayet, J.-F., Lieke, K., Kandler, K., Ebert, M., Weinbruch, S., Stohl, A., Gasteiger, J., Groß, S., Freudenthaler, V., Wiegner, M., Ansmann, A., Tesche, M., Olafsson, H., and Sturm, K. (2010), Airborne observations of the Eyjafjalla volcano ash cloud over Europe during air space closure in April and May 2010, *Atmos. Chem. Phys*., 11, 2245-2279, doi:10.5194/acp-11-2245-2011.

Stohl, A., A.J. Prata, S. Eckhardt, L. Clarisse, A. Durant, S. Henne, N. I. Kristiansen, A. Minikin, U. Schumann, P. Seibert, K. Stebel, H.E. Thomas, T. Thorsteinsson, K. Tørseth, and B. Weinzierl (2011), Determination of time- and height-resolved volcanic ash emissions and their use for quantitative ash dispersion modeling: the 2010 Eyjafjallajökull eruption. *Atmos. Chem. Phys*., 11, 4333–4351.

Tesche, M., P. Glantz, C. Johansson, M. G. Norman, A. Hiebsch, P. Seifert, A. Ansmann, R. Engelmann, and D. Althausen (2012), Volcanic ash over Scandinavia originating from the Grímsvötn eruptions in May 2011, *J. Geophys. Res*., doi:10.1029/2011JD017090.

Thomas, W., T. Erbertseder, T. Ruppert, M. van Roozendael, J. Verdebout, D. Balis, C. Meleti, and C. Zerefos (2005), On the Retrieval of Volcanic Sulfur Dioxide Emissions from GOME Backscatter Measurements. *J. Atmos. Chem*., Vol. 50, pp. 295-320.

Thomas, H. E. and Prata, A. J (20011), Sulphur dioxide as a volcanic ash proxy during the April–May 2010 eruption of Eyjafjallajökull Volcano, Iceland, *Atmos. Chem. Phys*., 11, 6871-6880, doi:10.5194/acp-11-6871-2011.

Valks, P., D. Loyola, N. Hao, M. Rix, and S. Slijkhuis (2011), ATBD for GOME-2 total columns of ozone, $NO_2$, $SO_2$, BrO, $H_2O$, tropospheric NO2 and cloud properties, *Rep. DLR/GOME-2/ATBD/01, 2/E,* Earth Observ. Cent., Wessling, Germany, 23 March. [Available at http://atmos.caf.dlr.de/gome2/docs/DLR_GOME-2_ATBD.pdf.]

van Geffen, J, M. Van Roozendael, M. Rix, P. Valks, (2008), Initial validation of GOME-2 GDP 4..2 $SO_2$ total columns (OTO/SO2) – ORR B, 2008, TN-IASB-GOME2-O3MSAF-SO2-01.1 available at http://o3msaf.fmi.fi/valreps.html.

Witham C.S, Hort M.C, Potts R, Servranckx R, Husson P, Bonnardot F. (2007), Comparison of VAAC atmospheric dispersion models using the 1 November 2004 Grímsvötn eruption. *Meteorol Appl* 14: 27–38.

WMO (2008), Recommendations for the verification and intercomparison of QPFs and PQPFs from Operational NWP Models, *WMO/TD* – No. 1485.

Yang, K., X. Liu, N.A. Krotkov, A.J. Krueger, S.A. Carn (2009), Estimating the altitude of volcanic sulfur dioxide plumes from space borne hyper-spectral UV measurements, *Geophys. Res. Lett.,* Vol. 36, doi:10.1029/2009GL038025